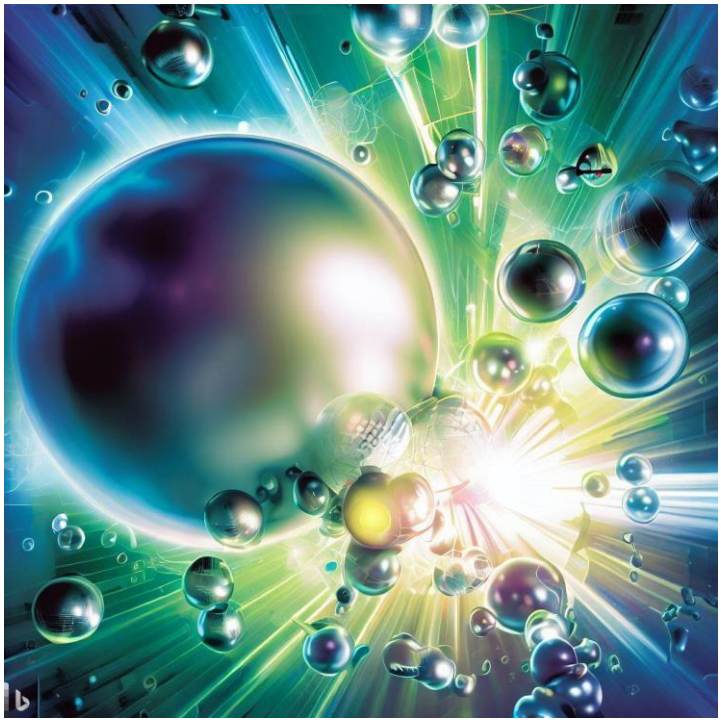

MAX IV and Wallenberg Initiative Materials Science for Sustainability (WISE)

Summary of Existing Capabilities

2023-04-17

MAX IV LABORATORY

Contents

Contributors:

Stefan Carlson
Mads Jørgensen
Samuel McDonald
Erik Mårsell
Aymeric Robert
Andrey Shavorskiy

Front page artwork: AI generated image from the prompt “Cover art for sustainable materials science with synchrotrons”.

1. Introduction

MAX IV is heavily supporting current materials science research in Sweden and internationally. The facility currently has 16 operational beamlines serving a community of approximately 50% Swedish and 50% international users. Over the past few years, MAX IV has received a steadily increasing number of proposals, and now has an average oversubscription rate close to 2. In addition to academic research, MAX IV also offers proprietary beamtime for industrial users, delivering over 500 hours of beamtime annually in this segment.

Our beamline portfolio offers experimental capabilities relevant for a wide range of materials science. The purpose of this document is to present relevant examples of scientific experiments that either have been done or can be done with the currently available techniques, and how they align with the WISE initiative.

To illustrate how the research capabilities of MAX IV fit into the WISE Initiative focus areas, we use the WISE matrix (Figure 1.1). Generally, MAX IV activities focus on the rows b-d, although closely interacting with activities tied to rows a and e through collaboration and exchange of information. To give specific examples of how MAX IV can contribute through current capabilities, this document is divided into the three categories Scattering and Diffraction, Spectroscopy, and Imaging.

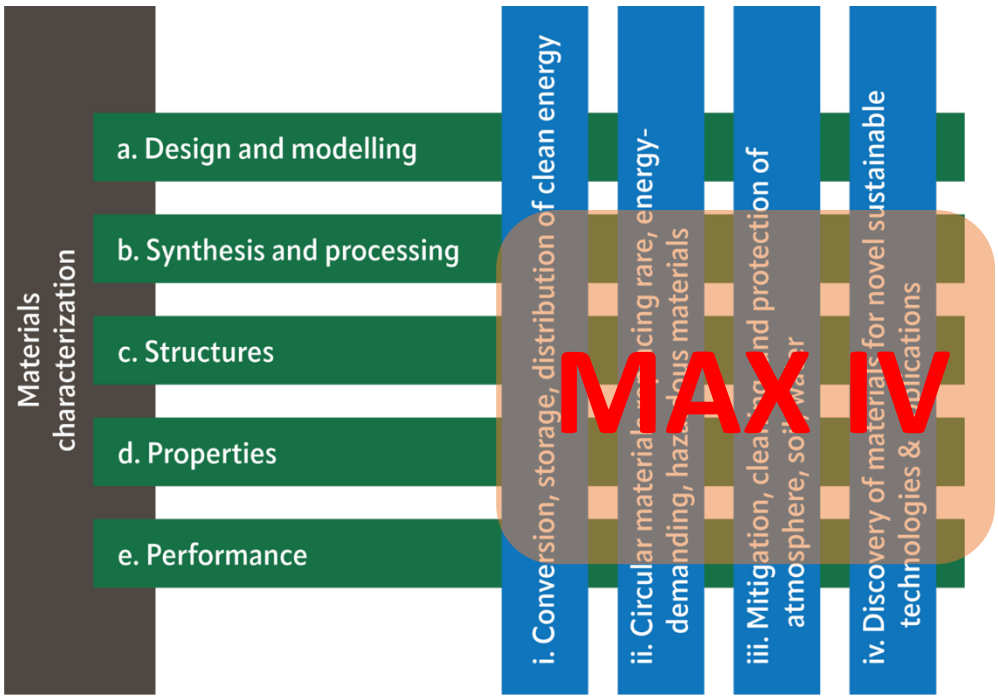

Figure 1.1. The WISE matrix of research areas, with the areas mostly covered by current MAX IV activities shown.

2. Scattering and Diffraction

The relevant beamlines for scattering and diffraction in WISE are: Balder (X-ray absorption/emission spectroscopy and X-ray diffraction), CoSAXS (Small angle X-ray scattering, also available at ForMAX) and DanMAX (Powder X-ray diffraction and Total Scattering). Balder is included here due to its combination of spectroscopy and diffraction capabilities, but could also be included in the spectroscopy section. DanMAX is included both here and under the imaging section due to its separate diffraction and imaging end stations. FemtoMAX is also a scattering and diffraction beamline, however, due to its very different time resolution it is not grouped with the other storage ring-based beamlines.

WISE related activities at these beamlines can be grouped into the following categories, spanning material characterization from synthesis (b) to performance (e) for all material areas (i-iv):

1. ***In situ*** **synthesis investigations:** The complexity of novel, tailor-made materials, often containing several different elements, increases the complexity of synthesis processes. Good knowledge of synthesis processes, including all kinetics and intermediate stages, enables a knowledge-based tuning of specific material properties and the development of green and scalable production processes. Applying multimodal *in situ* approaches, we enable to discover structure (WISE area c)–property (d) relationships during synthesis and processing (b) with time resolution down to sub-seconds. For specific materials, e.g. for photovoltaics, synthesis investigations can even contain performance aspects (e), by auxillary measurements, such as catalytic performance by mass spectroscopy or photovoltaic conversion efficiency by photoluminescence.
2. ***Operando*** **investigations:** For energy conversion and storage materials, it is of foremost importance to directly relate structures (c) and properties (d) to performance (e) and efficiency of devices. The hard X-ray beamlines, especially Balder and DanMAX, allow to discover such relations directly *operando* in model systems and industrially relevant devices. In multimodal XAS + XRD (or XRD + UV-vis) based experiments, performance measures such as the conversion efficiency of catalysts or cycling efficiency of batteries can be directly related to ongoing structural and chemical transforms during the operation of a device.
3. ***Ex situ*****, in-depth characterization:** Complex structure–property relations of novel materials are yet to be understood. Both Balder, CoSAXS/ForMAX, and DanMAX can provide high-quality, in-depth characterization of the chemical, structural and electronic material properties. These can e.g. be performed at cryogenic temperatures to increase signal-to-noise ratios or deconvolute thermal structural effects. The intense beam further allows to access and characterize very diluted species or small impurities in a majority phase.

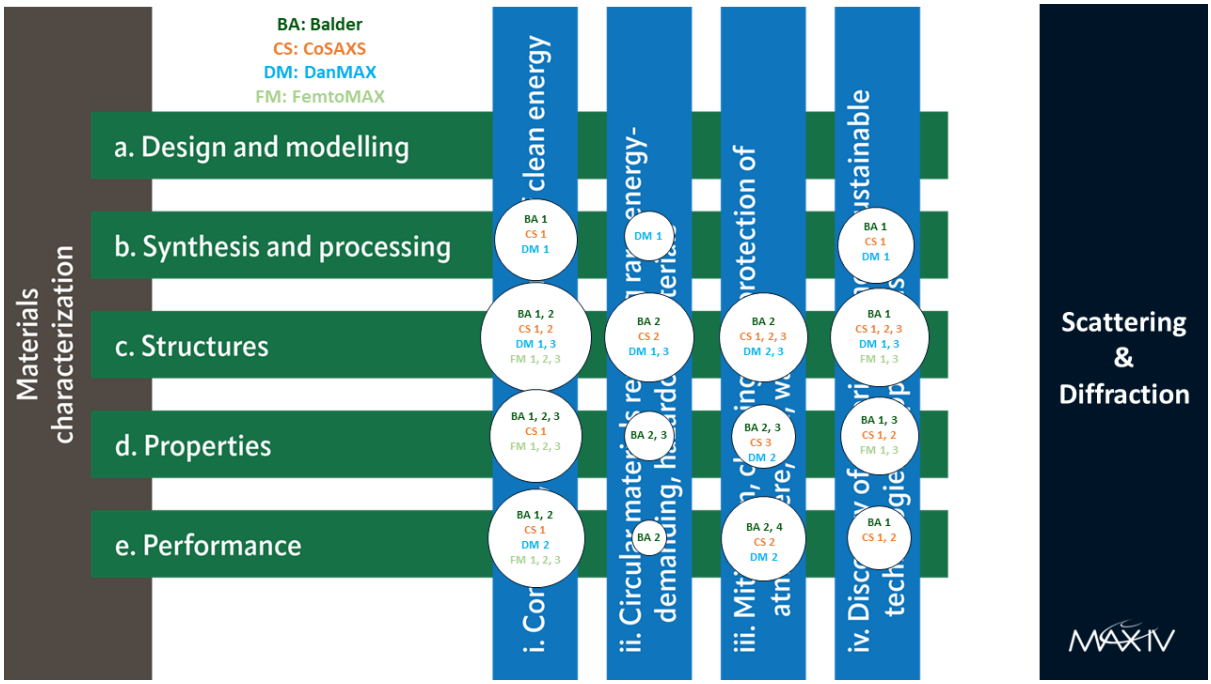

Figure 2.1. The WISE matrix of research areas, with specific examples from the scattering and diffraction beamlines shown and labelled.

2.1 Balder

Balder allows for multi-perspective, real-time investigations of materials and processes, combining high-flux and low divergence with quick and stable energy scanning. Simultaneously combining fast X-ray absorption spectroscopy (XAS, XANES, EXAFS) with X-ray diffraction (XRD), X-ray emission spectroscopy (XES) and further auxiliary techniques (mass spectroscopy, UV-vis, photoluminescence, Raman spectroscopy) we enable to determine the chemical, crystallographic, and electronic structure simultaneously, *in situ* during synthesis, processing and operation of materials.

Specific examples of different research areas are given in the following:

BA 1.1: i, iv | b, c, d, e: With the in-FORM (*in situ* platform for formation of energy materials) platform at Balder, we enable multimodal XAS-XRD-optical investigations of **solvent based synthesis processes** with a high level of automation in a high-throughput robotic synthesis device. The system was recently applied to discover kinetics and intermediates in the **synthesis of metal–halide perovskites for photovoltaic applications.** A fine-tuned process yielding world-record power conversion efficiency solar cell devices was adopted to *in situ* processing. Using a multimodal approach, we were able to follow the nucleation and growth of mixed Br-I material with element selectivity to determine how inhomogeneity can arise from processing conditions. While XAS reveals the element specific details of the solvent species, it is complemented by crystallographic information from XRD about the solid state. This allows to draw a comprehensive picture of the full process, from solvent over intermediates to the final metal–halide perovskite thin film. Simultaneous measurements of the photoluminescence allow to deduce the quality of the material *in situ* during synthesis, giving a quantitative estimate of the open-circuit voltage of the final device. This bridges all WISE characterization areas from synthesis (b) over structures (c) and properties (d) directly to performance (e) in one experiment and thus demonstrates how material research and developments could be accelerated. This methodology of high-throughput *in situ* experiments is further very promising for the discovery of new materials and greener processes. Manuscripts are currently in preparation. Collaboration with group of E. L. Unger, Humboldt University Berlin.

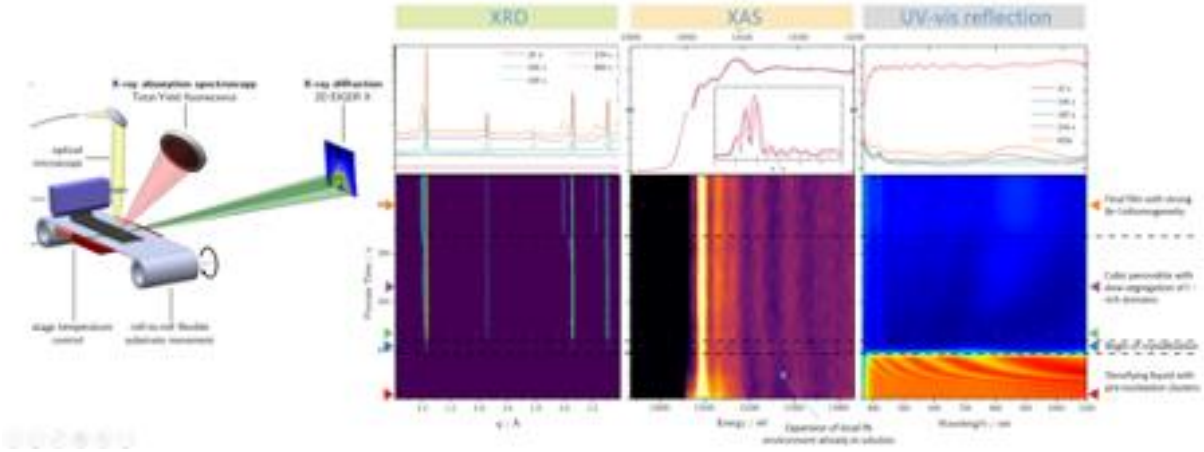

Figure 2.1. *In situ* solution processing of perovskites for photovoltaics: Formation of FA,MA $Pb(I,Br)_3$ perovskites. A similar process from collaborators (group of E. L. Unger, Lund University / Humboldt University Berlin) yields world record efficiency devices (20.8 %). (Li *et al.*, 2021)

The in-FORM setup has so far only been used for metal-halide perovskites, but should be applicable for any solution-solid reaction at temperatures under 400 °C.

BA 1.2: i | b, c, d: Among the large family of metal–organic frameworks (MOFs), **Zr-based MOFs** are foreseen as one of the most promising classes of MOFs for practical applications in **catalysis** due to their rich structure types, outstanding stability, and intriguing properties and functions. *In situ* XAS measurements have been used to follow the growth of MOFs during hydrothermal synthesis. This allowed to deduce process kinetics and identify the local environment around Zr^{4+} in the early, pre-crystalline, stages of Zr-MOF synthesis utilizing various inorganic cluster precursors. Manuscript in preparation (group of O. Zavorotynska, University of Stavanger).

BA 1.3: i | b, c, d: The exact size and shapes of **nanocrystals** determine their functional properties **in energy conversion and storage applications**. Binary, ternary, and multinary nanocrystals often have complex synthesis procedures, involving the formation and decomposition of several intermediate stages. These can be unravelled combining complementary information about precursors in solution from XAS with details about the crystalline state from XRD in multimodal experiments at Balder, where different *in situ* cells for hydrothermal synthesis are available.

Examples of projects are:

a. *Formation of metal alloy nanoparticles from parent perovskite oxide followed by in situ XAS*: Exsolution of metal nanoparticles from perovskite oxides is a novel strategy to prepare supported catalysts. Combining XANES and EXAFS allowed for simultaneous detection of element specific changes in the short-range order and valence status of both elements (group of S. Mascotto, Hamburg University).
b. *Nucleation and growth of colloidal quaternary nanocrystals:* Copper chalcogenide nanocrystals find applications in photovoltaic inks, bio labels, and thermoelectric materials. Insights into the nucleation and growth during synthesis of anisotropic Cu_2ZnSnS_4 nanocrystals are gained by combining X-ray absorption and scattering. Collaboration with group of K. Ryan, University of Limerick, Ireland (measurement not performed at Balder, however would now be possible).
c. *Mechanism for MoO_2 nanoparticle formation studied by in situ XANES:* Molybdenum oxide nanocrystals show a very rich structural chemistry with a range of stable structures and stoichiometries, which all have different properties for use in e.g. catalysis or as battery

electrodes. *In situ* XAS experiments during hydrothermal nanoparticle synthesis enable to identify the reduction mechanisms and changes in local structure that direct the formation of MoO_2, exhibiting either the HP-MoO_2 or the distorted rutile structure as well as the formation of defects within this structure (group of K. M. Ø. Jensen, University of Copenhagen).

BA 2.1: ii | c, d, e: **Catalysts and their supports for application in H_2 production, fuel cells or CO_2 hydrogenation** often undergo transformations under operation conditions, significantly influencing their catalytic activity. A detailed mechanistic understanding of all processes and interactions between support, catalyst, and the reactants is therefore needed for the development of new, highly efficient, and abundant catalysts. Balder offers sample environments for multimodal XAS-XRD *operando* investigations at various temperatures with possibilities for auxiliary measurements of e.g. mass or Raman spectroscopy. A comprehensive gas mixing and supply infrastructure for such experiments will soon be implemented. Examples of projects are:

a. *Elucidating the chemical state and the reaction intermediates of Fe and Cu based catalysts for CO_2 hydrogenation by simultaneous operando Raman and X-ray absorption spectroscopy:* Here, the catalytic nature of Fe and Cu-based nanocatalysts under CO_2 hydrogenation conditions as function of the structure, nanoparticle size, and support has been investigated through XAS. Simultaneously collected Raman spectroscopy provided complementary information on chemical intermediates and phases involved during the catalytic cycle. Manuscript in preparation (group of B. R. Cuenya, Fritz-Haber-Institute, Berlin).
b. *Elucidating MOF catalyst structure during electrocatalytic CO_2 reduction:* Multimodal, *in-operando* XAS-XRD characterization of the structure–activity relationship of metal–organic framework (MOF) based catalysts for the electrochemical CO_2 reduction (Frank *et al.*, 2021; experiment during fall 22).

BA 2.2: ii | c, d, e: Energy storage devices such as **lithium ion batteries** are exquisitely complex chemical systems with multiple components interacting in ways dependent on the operating conditions. The intertwined reactions subsequently create changes that manifest over multiple length and time scales affecting battery lifetime and safety. Here we combined XAS, XRD, and anomalous XRD to investigate the complex interplay between electrochemical reactions and phase transformations ***operando*, during the cycling of a battery**. Collaboration with group of W. Brant, Uppsala University, manuscript in preparation.

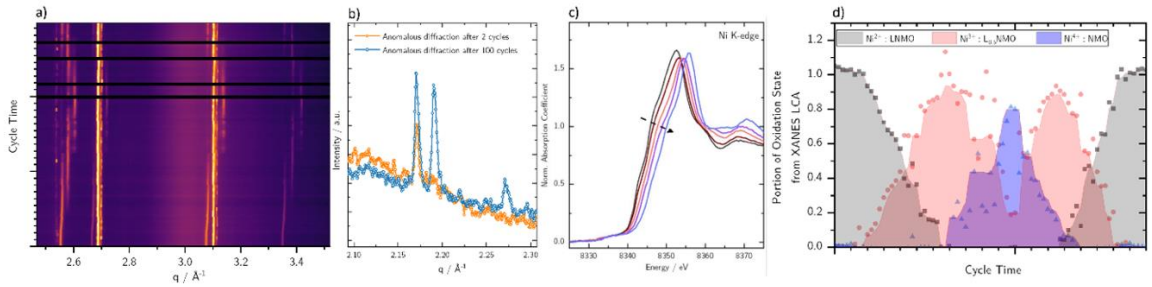

Figure 2.2. Combined *operando* scattering and spectroscopy data from Balder during the cycling of a battery.

BA 2.3: iii, iv | c, d, e: To **close the plastic recycle loop** CO_2 from incineration of plastic waste should be captured and made into new plastic. Global aim is here the conversion of CO_2 into plastic monomers, such as light olefins. To do this, the CO_2 can be combined with hydrogen, which can be obtained from water electrolysis, to form a so-called synthesis gas, which can be converted to methanol, which can further be converted to olefins in the methanol to olefins (MTO) process. Here

the active sites of high temperature methanol synthesis catalysts based on zinc oxide and indium oxide were investigated under *operando* conditions by XANES and EXAFS. Balder offers an *in situ* reaction cell for *operando* characterization of catalysts under industrially relevant conditions (here: 400 °C, 25 bar, gas flow of CO, CO_2, H_2, syngas). Group of M. Hoj, DTU Copenhagen, manuscript in preparation.

BA 2.4: iv | c, d, e: **Methane** is 84 times more potent than carbon dioxide as a greenhouse gas and is **emitted from power generation**, diesel and compressed natural gas engines, gas wells, etc. To **mitigate the emission of methane**, it can be catalytically converted to CO_2 and H_2O. Here, we investigated the interplay between nanocrystalline Pd catalysts, supported on alumina, and the gas phase, *operando* under different reaction conditions by simultaneously applying XAS and XRD together with performance measurements by mass spectroscopy. Our results reveal the oxidation of Pd nanocrystals in two clear stages with different activation energies for surface and bulk oxidation.

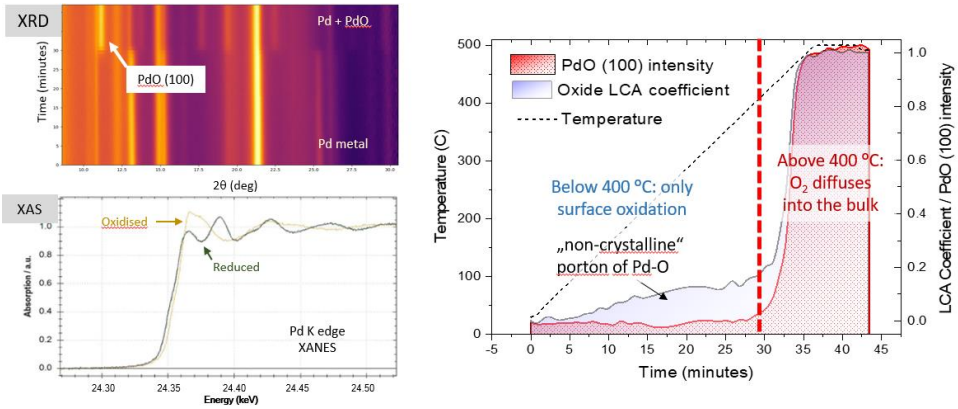

Figure 2.3. Multimodal *operando* experiments on Pd nanocrystals during methane conversion into CO_2 and H_2O under operando conditions at Balder. While XAS reveals the overall contribution of oxidized Pd atoms, XRD detects the crystalline portion of PdO. In combination, the non-crystalline portion of PdO is revealed. Collaboration with group of P.-A. Carlsson, Chalmers University of Technology, Göteborg, manuscript in preparation.

BA 3: i, ii, iii, iv | d: There are numerous examples of ***ex situ*, in-depth investigations** on materials for sustainability at Balder. Examples of projects are:

a) *Reversible Atomization and Nano-Clustering of Pt as a Strategy for Designing Ultra-Low Metal Loading Catalysts:* Detailed EXAFS investigations show that the Pt-state is reversibly changed between single atomic sites in Mg antisite vacancies and strongly anchored small clusters, when treated in high temperature oxidizing and reducing conditions (Chakraborty *et al.*, 2022).

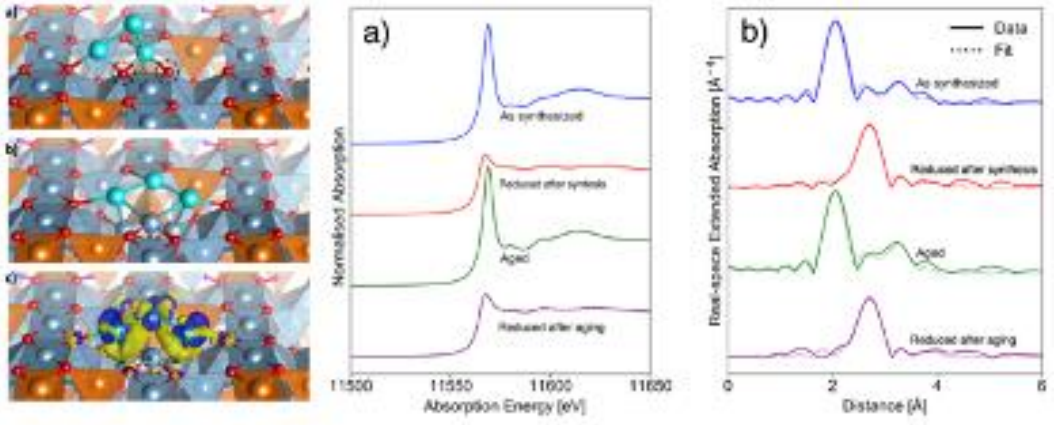

Figure 2.4. Local atomic structure of catalytically active Pt-sites from DFT and XAS perspectives.

c) *Highly Stable Apatite Supported Molybdenum Oxide Catalysts for Selective Oxidation of Methanol to Formaldehyde: Structure, Activity and Stability:* Detailed XANES and EXAFS analysis for detection of oxidation states and surface/amorphous MoO_x species before and after exposure to reaction conditions (group of M. Hoj, DTU Copenhagen).

BA 4: iii | e: Incineration is in many countries a common treatment method for municipal solid waste, and **utilization of the ash residues** has attracted significant interest. The bottom ash is best suited as a secondary construction material, whereas the fly ash is being investigated as a secondary raw material for recovery of, for example, Zn, Cu, and salts. For both types of application, knowledge about the chemical speciation of Zn and Cu in the ashes is valuable. Systematic investigation of samples from fly ash and bottom ash from three waste-to-energy plants using XANES reveal the chemical forms that Cu and Zn appear in (Rissler *et al.*, 2020).

2.2 CoSAXS (and ForMAX)

The CoSAXS beamline is a multipurpose Small Angle X-ray Scattering (SAXS)/Wide Angle X-ray Scattering (WAXS) instrument with opportunities to use the inherently high coherence of the 3 GeV MAX IV ring through X-ray Photon Correlation Spectroscopy (XPCS) experiments. The high-performance X-ray beam is complemented by a large pool of sample environments and detector systems. Several techniques are available through modular operation: time-resolved SAXS, SAXS/WAXS, protein solution SAXS, micro-focusing SAXS, anomalous X-ray scattering and XPCS. ForMAX additionally complements the scattering with tomographic imaging of the sample to extend the length scales under study from millimetres to nanometres. It is further capable of SAXS/WAXS tensor tomography yielding isinght into the hierarchical nature of many important materials.

Specific examples of different research areas are given in the following:

CS 1: i, iv | b, c, d, e: The properties of nanomaterials are intimately linked to the size and morphology of the particle structure of the material. In organic solar cells, for example, the active layer for energy conversion is typically a self-assembled, heterogeneous mixture of two components, a polymer and a fullerene, which for maximum efficiency need to be segregated on the length scale of 5 to 10 nm. The SAXS/WAXS technique at CoSAXS can determine the nanomorphology of these materials, and this information has the potential to boost the performance, capacity and stability of organic photovoltaics (Yang *et al.,* 2020; Xia *et al.,* 2021).

Potential development: Many of the fuel and energy conversion/storage cells involve thin films and layers. Grazing incidence SAXS and WAXS (GISAXS/GIWAXS) would be necessary for better characterization of these devices. *Operando* investigation would be possible with appropriate modification of the fuel cells.

CS 2.1: iv | c, d, e: New increased efficiency and targeted catalysts are transforming green energy production. Understanding catalytic mechanisms and performance will require multidisciplinary and *operando* approaches. Synchrotron SAXS measurements at CoSAXS can contribute through providing nanostructural information during, for example, the degradation of the catalysts or the changes in an electrode of a fuel cell in operation (Mochizuki *et al.,* 2014; Povia *et al.,* 2018; Tsao *et al.,* 2007).

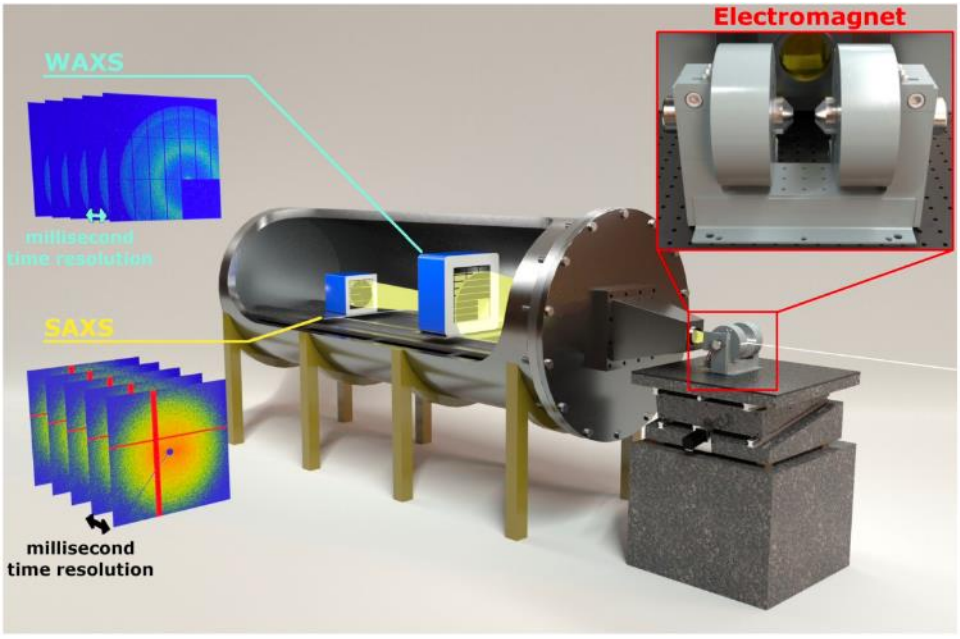

Figure 2.5. Experimental setup at CoSAXS to follow the *in situ* response of metallic nanoparticles to external magnetic fields.

CS 2.2: iii | c, e: There are several methods used in the water purification process from filtration, (e.g. using activated carbon), sedimentation (flocculation), or distillation and the use of ultraviolet light. *In situ* SAXS studies will help in optimization of such processes and in the quantification of impurities and residues (Bone, Steinrück, and Toney, 2020; Maison *et al.*, 2000).

Potential development: Combining multiple synchrotron techniques as well as multimodal methods is clearly required to fully understand the evolution of nanostructures occurring in many of the examples noted above. The SUrF (SAXS, UV-vis, Raman, and Fluorescence) platform under development at CoSAXS could be extended to combine spectroscopy measurements within an *operando* device, rather than a glass capillary holding the sample.

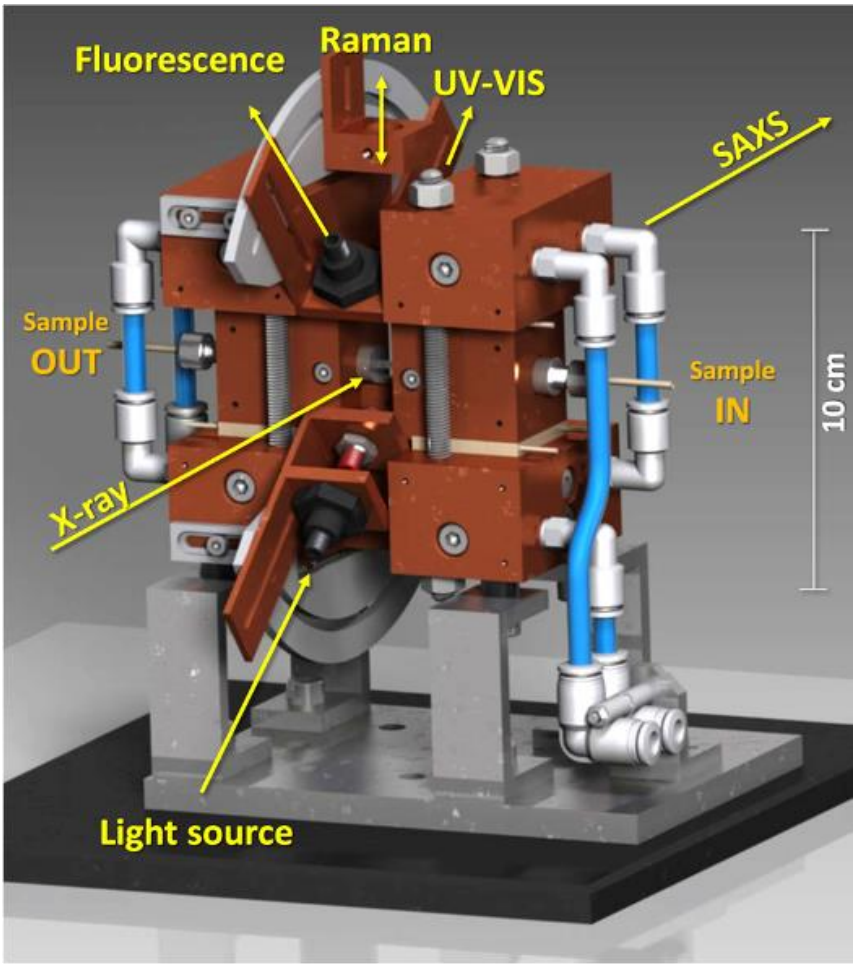

Figure 2.6. SUrF equipment allowing simultaneous SAXS, UV-Vis, Fluorescence and Raman of samples in a glass capillary. The spectroscopy probes are coupled to the SAXS measurements through the use of fibre optics.

CS 3.1: iii | c, d: Quantifying structures in soils: Soils and clays are nanostructured materials, with the aggregates in the soil exhibiting a fractal nature. Soils with high organic carbon content are being examined for their potential as sinks for greenhouse gases. SAXS gives information on the compactness (fractal dimension) and porosity forming the soil structure (Guénet *et al.,* 2017; Tsukimura and Suzuki, 2020).

CS 3.2: iv | c: Cellulose based materials for sustainable technologies constitute a key research field of the Wallenberg Wood Science Centre. A recent development is the ability to developed conducting cellulose yarns that can be used for making electronic textiles (Darabi et al, 2022). Functional composite materials from forest-based and other polymer-based materials will be eco-friendly and have application in high-performing energy, electronics, and photonics technology. Characterization of the molecular orientation in these complex composite with SAXS/WAXS and tomographic imaging will be essential to fully exploit their application.

2.3 DanMAX (Diffraction)

DanMAX is a materials science beamline focusing on *in situ* and *operando* studies of all types of materials. The main techniques employed are X-ray diffraction and Total Scattering for local and long-

range atomic structure determination, X-ray fluorescence for elemental mapping and full field imaging. In this section we show examples of diffraction and scattering. Imaging examples are included in a later section of this document. A focal point for the beamline is development of advanced sample environments in collaboration with the user community. Several of these are already available for the general users (e.g. battery cycling, solvothermal synthesis, high and low temperatures, gas loading, high pressure) and more are being developed, tested and commissioned (e.g. ultra-rapid sintering, high pressure and heating, humidity).

Specific examples of different research areas are given in the following:

DM 1.1: ii | b, c: Ultra-fast sintering of rare earths free magnets. Strontium hexaferrite nanoplatelets will align during compaction and allow for higher energy product than conventional ferrite magnets. Ultra-fast sintering is thought to retain a small particle size which retains the desirable magnetic properties of the nanostructured precursor. *In situ* ultra-fast sintering allows a detailed view into the bulk of this process and thus allows the researchers a better understanding of this last, but crucial synthesis step. This method is not only applicable for magnets, but for many other inorganic materials synthesized at high temperatures, e.g. lead free piezoelectrics. DanMAX will get an updated version of the furnace capable of sintering at temperatures up to 1500 K and heat rates of up to 150 K/s in the spring of 2023 (Shyam *et al*., submitted; Gjørup *et al*., in preparation).

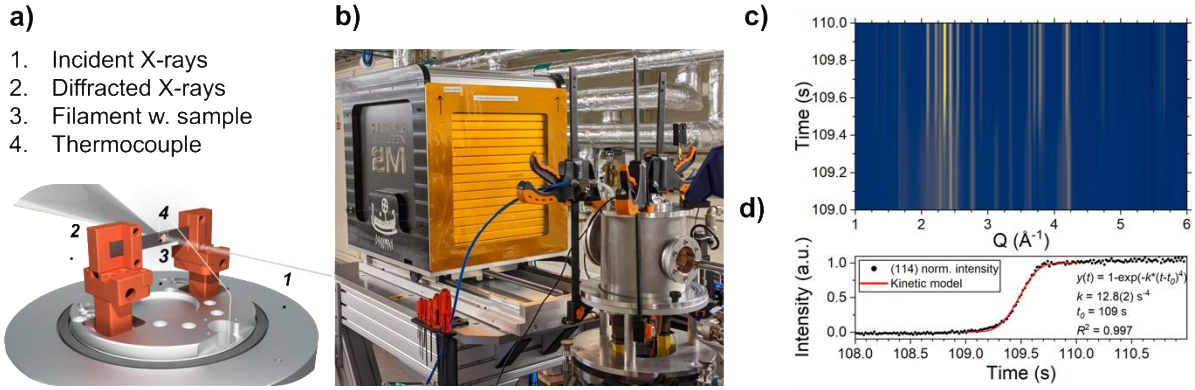

Figure 2.7. Aarhus Rapid Ohmic Sintering (ARΩS) furnace at DanMAX. a) Schematic view of the furnace. b) Furnace installed at DanMAX during commissioning. c) PXRD data recorded over 1 second at 250 Hz during calcination of ferrihydrate. d) Integrated intensity of the 114 reflection fitted with a kinetic model (Gjørup *et al*., in preparation).

DM 1.2: i, ii, iv | b, c: *In situ* solvothermal synthesis of nanomaterials. Properties of nanomaterials are intimately linked to the size and morphology of the particles, which depend on the synthesis conditions. Nanomaterials are a staple of modern technology and used in e.g. energy storage, energy conversion, and catalysis. To both develop new materials and greener ways to produce these, a very large parameter space will need to be mapped out. This can to a certain extent be performed using flow synthesis in a lab with *ex situ* examination of the products. *In situ* XRD and PDF analysis during a reaction allow for a 'live view' inside the reactor that can follow the formation of the nanomaterials and 'see' how precursors and metastable intermediate compounds lead to the final product. At DanMAX we have a reactor capable of hydrothermal synthesis at supercritical and near-critical conditions. This allows for a green synthesis route in a benign solvent (Broge *et al*., 2022; Roelsgaard *et al.*, submitted).

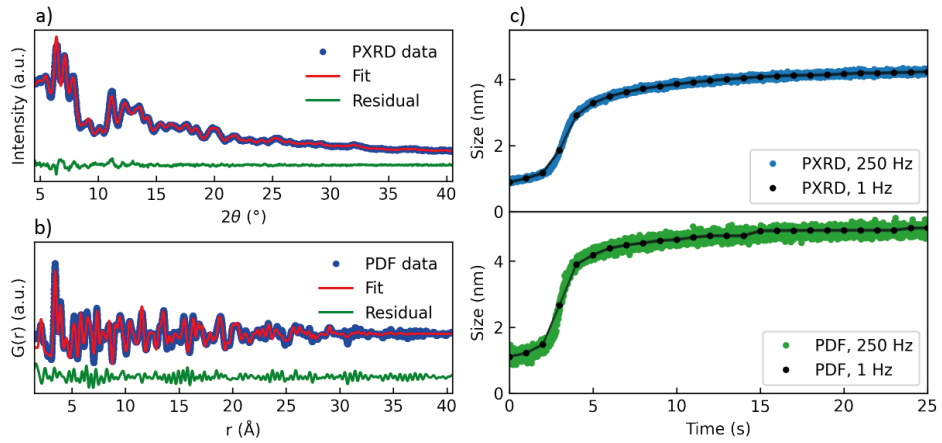

Figure 2.8. Solvothermal synthesis of HfO_2 nanocrystals. a) PXRD data (blue), Rietveld model (red) and difference curve (green). b) Experimental Pair Distribution Function (blue), refined structural model (red) and difference curve (green). c) Refined apparent nanocrystal size as a function of reaction time derived from PXRD (top) and PDF (bottom) (Roelsgaard *et al.*, submitted).

Potential development: Integration of the In-FORM slot die coating sample environment at DanMAX (and other MAX IV beamlines). Continued development of the slot die coater at BALDER would allow it to be used at several other beamlines at MAX IV. This would allow for (like the use at BALDER) to map out a very large synthesis parameter space to optimize thin film production of basically any solvent-solid state reaction under 400 °C.

DM 2.1: i | c, e: *Operando* testing of batteries. The chemistry in an operating battery is far from equilibrium. Thus information about chemistry and structure of the constituents must be collected during operation for a comprehensive understanding of the charge/discharge processes. This is also the best way to elucidate on and the mechanisms leading to degraded performance over time. At DanMAX we can simultaneously cycle 8 batteries while collecting XRD data on each approximately every 150 s (Christensen *et al.*, accepted; Graae *et al*., submitted).

Potential development: Expanding the capacity for battery experiments with a very high-capacity battery cycler (~100 cells) and advanced software for automatic experimental feedback. This would allow ideal conditions for machine learning models relating battery performance and structure/XRD data. The battery cycler could be developed to fit multiple MAX IV (hard X-ray) BLs

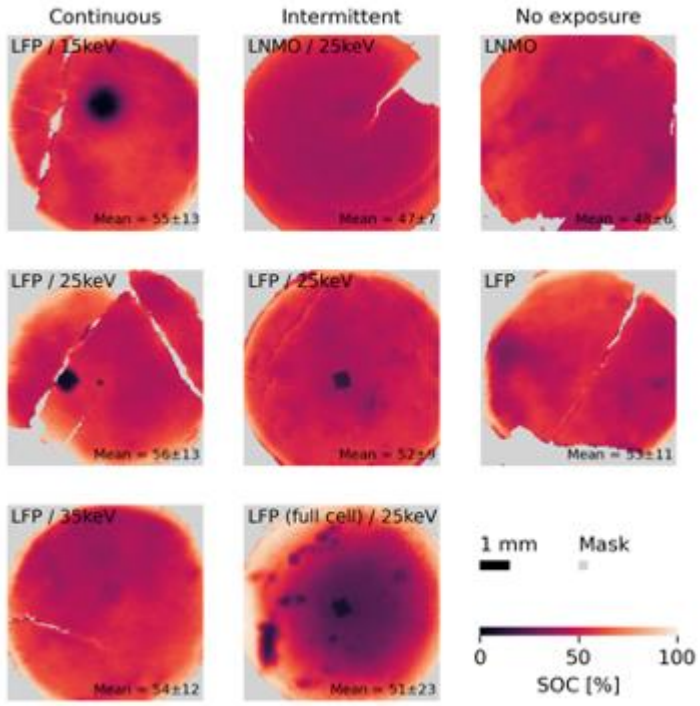

Figure 2.9. State of Charge (SOC) maps of battery electrodes. A range of batteries were subjected to varying X-ray exposure and photon energies while being charged. The battery stack was subsequently mapped with spatially resolved µXRD. Clear beam induced effects can be seen for e.g. $LiFePO_4$ at 25 keV both during continuous and intermittent X-ray exposure (Christensen *et al*., 2023).

DM 2.2: iii | c, d, e: Multimodal *operando* characterization of catalysts. Catalysts are of tremendous importance in many chemical reactions performed at scale and will be even more important in the green transition. A comprehensive understanding of the catalytic mechanism and performance requires a multidisciplinary approach. A useful tool to obtain structural understanding during operation is XRD. Since XRD does not yield direct information about e.g. gases and liquids in the catalyst it can be coupled with e.g. mass spectrometry (MS) to analyse the performance of the material. It can further be combined with UV-vis (or IR) spectrometry for even more information about the system. At DanMAX we have performed one experiment combining all of these techniques, however, the gas system, mass spectrometer, and UV-vis spectrometer were all brought by the users and are not available to general users. Experiments performed at DanMAX by the groups of S. Svelle, UiO, NO, and L. Lundegaard, Haldor Topsøe, DK. Manuscript in preparation.

Potential development: Strengthening catalysis research with integration of MS and UV-vis spectrometer. This could be developed as a portable solution that could be deployed at various MAX IV BLs for catalysis experiments. (A fixed general-purpose gas system is planned, but not yet implemented at DanMAX).

DM 3.1: i, ii, iii, iv | c: *Ex situ* / postmortem structural analysis using XRD or total scattering (PDF) analysis. This is the basic function of DanMAX and is covering all scientific field interested in the atomic structure of crystalline (or near crystalline) materials (see *e.g.* Anker *et al*., 2022; Grinderslev *et al*., 2022; Juelsholt *et al.,* 2021; Sandar Htet *et al.,* 2022) and even the structure of solvated ions in various solvents (Kløve *et al*., 2022;).

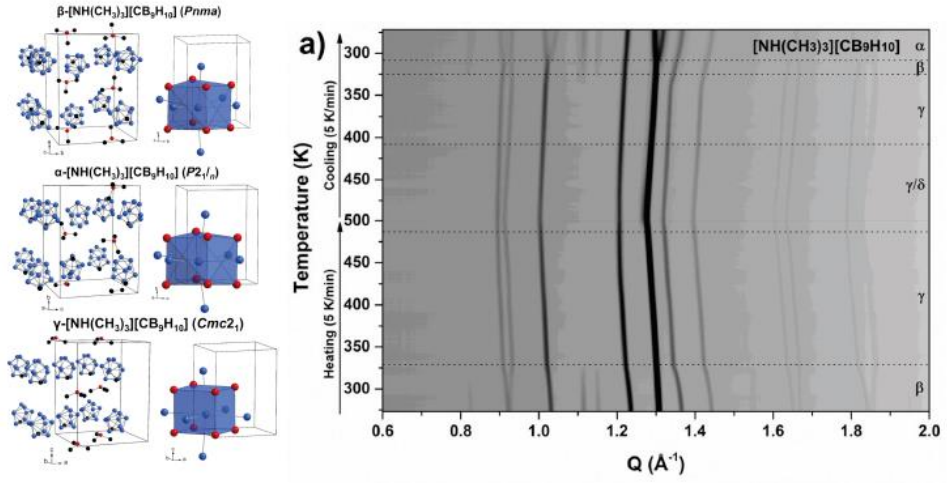

Figure 2.10. Left: Different polymorphs of $[NH(CH_3)_3][CB_9H_{10}]$ solved from PXRD data. Right: *In situ* multi temperature PXRD data from $[NH(CH_3)_3][CB_9H_{10}]$ measured from 273 to 500 to 273 K (5 K min^{-1}). Adapted from Grinderslev *et al*. (2022).

DM 3.2: iv | c: Structural studies of materials under high pressure. Discovery of new materials has always been a fascinating discipline in materials chemistry and continues to be of key importance for further advancements in materials science. Use of high pressure allows unique opportunities to stabilize new compounds with unusual atomic coordination and bonding – potentially with novel and desired properties. At DanMAX we have the infrastructure to measure XRD data under high pressure in diamond anvil cells (DACs), and further to measure XRD data on the miniscule amounts of sample commonly produced in high pressure (and high temperature) synthesis. (Ottesen, Petersen *et al*., submitted; Ottesen, Goesten *et al*., in preparation)

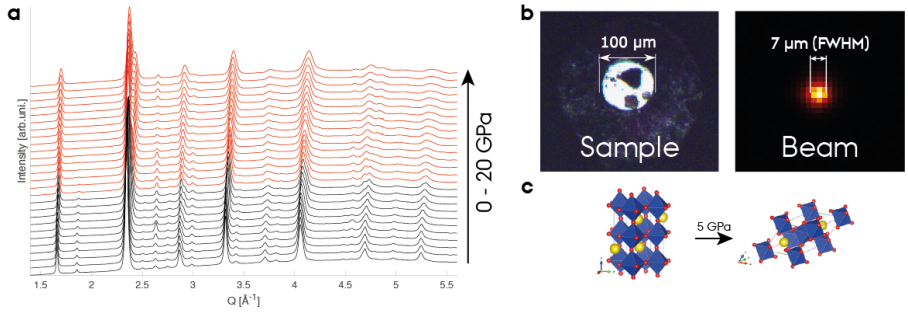

Figure 2.11. Pressure induced phase transformation of $PrCoO_3$. a) PXRD data plotted as a function of applied pressure. The black traces show the low pressure while red shows the high-pressure phase. b) Microscope image of the sample within the diamond anvil cell and an image of the X-ray beam. c) Atomic structures of the two polymorphs.

2.4 FemtoMAX

FemtoMAX is a time resolved beamline dedicated to study solids using X-ray diffraction and scattering techniques with a potential of studying liquid samples in the near future. A femtosecond pulsed, tuneable laser is used to excite bulk, thin film, or nanostructured materials to study fast phase transitions, energy capturing and transfer, and laser-induced strain propagations. The FemtoMAX beamline provide users with 200 fs time resolution and flexible sample excitation geometries with a possibility to tune X-ray energy from 2 keV to 14 keV. Together with broad time scans covering time range from femtoseconds to nanoseconds, FemtoMAX is fulfilling the needs coming from a broad user

community. There are two columns in the WISE matrix that fit particularly well with the FemtoMAX experimental set-up and beamline staff experience:

i. Conversation, storage, distribution of clean energy.
iv. Discovery of materials for novel sustainable technologies and applications.

Specific examples of different research areas are given in the following:

FM 1: i | c, d, e & iv |c, d: Studies of material phase transitions covers a broad research field where one type of studies is focused around understanding the process itself, with a goal to discover pathways where a material goes from one state to another. Another goal is to find new materials/phases with unique properties, by going from one phase to another. Often those transitions are triggered using intense laser irradiation when the sample is cold, heated, or studied under high-pressure conditions.

Laser energy deposition in strongly absorbing materials happens within the first 100 nm. The excited region might contain a new phase/material for a short time only and subsequently return to its initial state. The importance of phase transitions in ultrafast time scales has be shown by Zalden *et al*. (2019). The new phase often has unique properties and can, e.g., be used for phase change memory devices or implementing phase change artificial neurons behaving the same as the biological ones.

Control of material properties using laser beams has been demonstrated at FemtoMAX, where fast X-ray stitching using laser pulses has been employed to reduce X-ray pulse duration from 100 ps to 20 ps (Jarnac *et al.*, 2017).

FM 2: i | c, d, e: Ultrafast studies of laser energy deposition in a material after irradiation is of importance in understanding energy conversion and transfer pathways on short time scales, i.e. before the material returns to its equilibrium state. Energy conversion, storage, and transfer in matter affect not only the performance of energy recovery units such as solar cells or thermoelectric devices, but also material resistance to damage in processes such as cutting blades or heat shields in harsh environments (extreme heat/cold).

Bulk (3D) as well as advanced thin film or nanostructure (2D) materials is a perfect match for studies at FemtoMAX with high temporal as well as spatial resolution. Especially nanomaterials are interesting due to their unique properties and potential for new energy harvesting materials (Mingo and Broido, 2004). FemtoMAX staff studied nanomaterials and their properties previously using time resolved diffraction (Jurgilaitis *et al.*, 2014a).

FM 3: i | c, d, e & iv |c, d: The FemtoMAX beamline can also be used to study light absorption efficiency in bulk, thin film, or nanostructured materials. Light trapping efficiency affects the initial material response, which is studied with femtosecond time resolution. A highly tuneable (200 nm – 12 um) laser system offers versatile material excitation options. In addition, a range of experimental conditions is available such as in air/vacuum and cold/hot sample environments. Nanomaterials in particular, with their applications in solar energy harvesting and high temperature thermoelectrics, can benefit from these experimental capabilities at FemtoMAX. Work with time-resolved X-ray studies of nanomaterials was performed at the MAX-lab (Jurgilaitis *et al.,* 2014b), and this has recently been tested at FemtoMAX using the G-chamber endstation.

Name of the end-station	GIXS	STACK	G-chamber
Photo	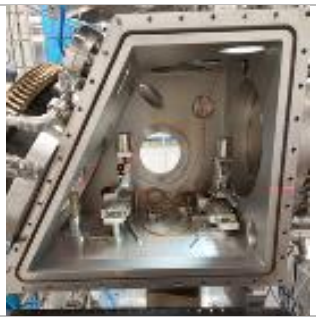		
Experi-mental data	1 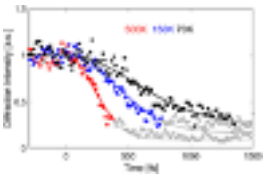 2 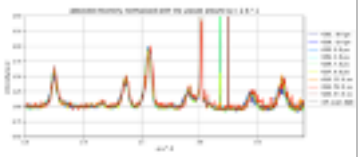	1 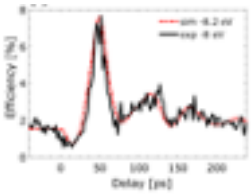 2 	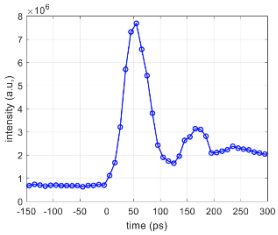
Reference	1. Wang *et al.* (2020), 2. Lorenc *et al.*, in preparation.	1. Jarnac *et al.* (2017), 2. Jensen *et al.* (2021).	Jurgilaitis *et al.*, in preparation.

Figure 2.12. The FemtoMAX endstations and some examples with references from experiments.

3. Spectroscopy

The use of spectroscopy, in particular electron spectroscopy, has been historically strong within the Swedish materials science community. MAX IV continues to support this community by providing a suite of beamlines offering X-ray Photoelectron Spectroscopy (XPS), Ambient Pressure XPS (APXPS), Angular Resolved Photoelectron Spectroscopy (ARPES), X-ray Absorption Spectroscopy (XAS), and Resonant Inelastic X-ray Scattering (RIXS) at the following beamlines at both storage rings: FlexPES (XPS, XAS), SPECIES (APXPS, RIXS, XAS), Bloch (ARPES), FinEst (XPS), Veritas (RIXS), HIPPIE (APXPS, APXAS), and Balder (XAS – see section 2 for detailed science cases). These beamlines provide experimental capabilities to enable the characterization of the following aspects of the materials:

- Synthesis. Understanding the process of material formation is the key to its successful commercialization. It is essential for complex multi-component, multi-layered materials where the interfaces between different compounds and phases might be influenced during the subsequent processing steps. The selection of sample environments is readily available at multiple spectroscopy beamlines to study materials synthesis in controlled environments and under real preparation conditions.
- Properties. X-ray spectroscopies provide rich information about the chemical and physical properties of materials under vacuum and at operational conditions. The availability of spectroscopy beamlines at both storage rings of MAX IV guarantees the techniques can operate with maximum efficiency (i.e., a combination of photon flux, energy resolution, and spot size), providing the best quality data in the shortest acquisition time. A large selection of sample environments implies that the MAX IV infrastructure is ready to investigate the properties of materials under ultra-high vacuum (UHV) as well as reaction conditions.
- Performance. Multimodal measurements, where the properties of the materials are characterized together with measurements of their performance, are an integral part of most sample environments at multiple spectroscopy beamlines. In addition, studying the mechanisms of the processes influencing material performance is another critical activity of the spectroscopy beamlines currently actively utilized by the materials science user community of MAX IV.

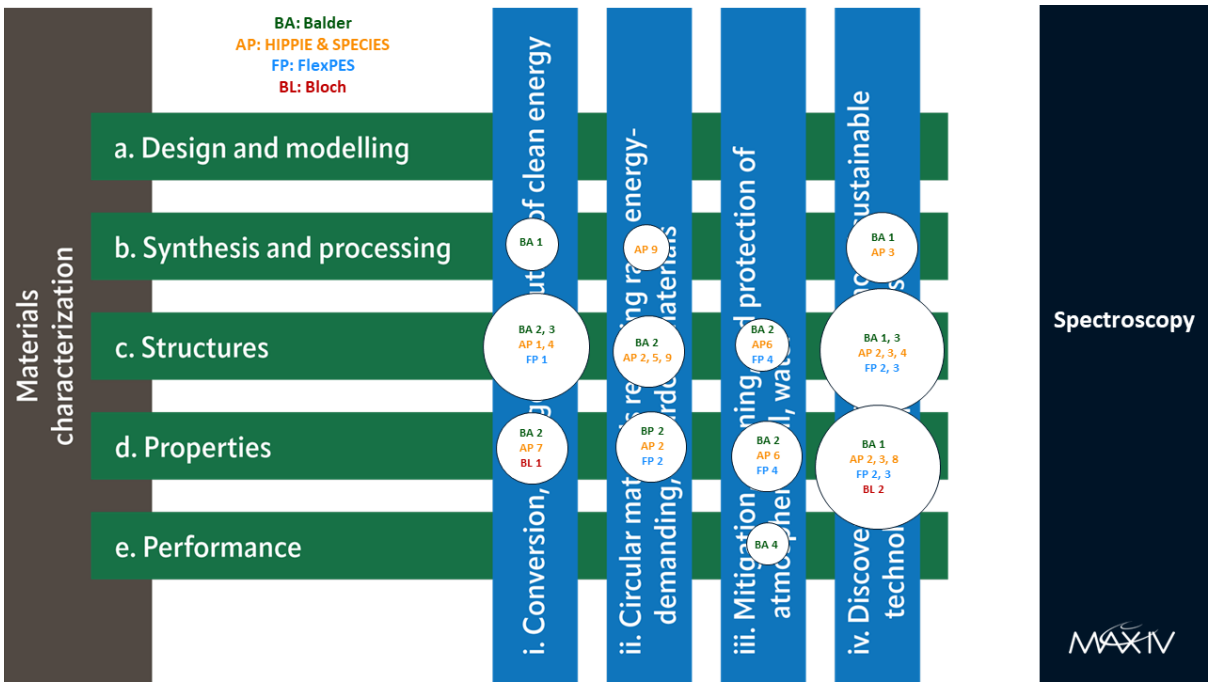

Figure 3.1. The WISE matrix of research areas, with specific examples from the spectroscopy beamlines shown and labeled.

3.1 APXPS (HIPPIE & SPECIES)

The Ambient Pressure X-ray Photoelectron Spectroscopy (APXPS) team consists of the HIPPIE and SPECIES-APXPS beamlines. The beamlines are designed to study the chemical properties of the interfaces between solids, liquids, and gases. The key characteristics of the beamlines – the high brightness in a wide energy range (30 eV – 2500 eV) and a selection of dedicated sample environments make them an ideal place for *operando* photoelectron spectroscopy applied to energy storage materials, photovoltaic systems, electro-, photo-, and thermal catalysts, corrosion-resistant multicomponent alloys, and thin-film growth by the atomic layer deposition.

Specific examples of different research areas are given in the following:

AP 1: i | c: In electrochemical energy storage devices such as batteries, essential electrochemical processes occur at the interface between the electrolyte and the electrode material. *Operando* APXPS is one tool to study these processes with chemical specificity, although accessing this crucial interface is not trivial. At HIPPIE, it is possible to probe the change in electrochemical potential over the solid/liquid interface of the working electrode even without direct access to the interface. Using this capability, researchers have shown that shifts in the kinetic energy of photoelectrons emitted from the electrolyte can be used to discriminate between the phase transition and lithiation/delithiation of a single phase in a $Li_4Ti_5O_{12}$ composite material.

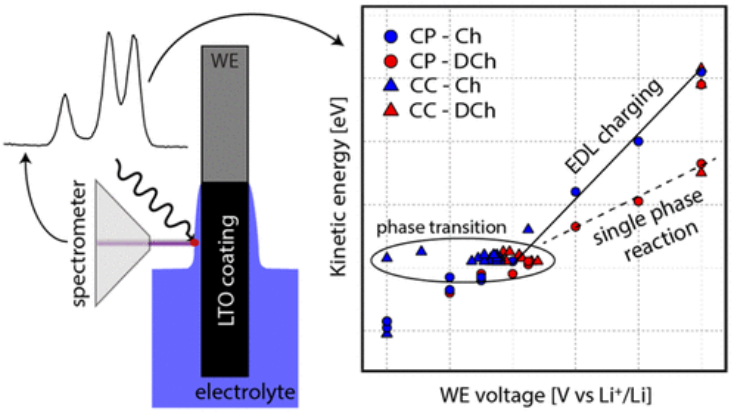

Figure 3.2. (Left) Illustration of the three-electrode setup used for operando APXPS measurements. (Right) The kinetic energy of the PC carbonate peak as a function of WE voltage during CC and CP cycling (Källquist *et al.*, 2022).

Examples of work: Källquist *et al.*, 2021; Källquist *et al.*, 2022; Maibach *et al.*, 2019.

Ongoing developments: Dedicated experimental platform for battery and corrosion research using APXPS at the HIPPIE beamline

Potential development: Quick *operando* XAS.

AP 2: ii | c, d & iv | c, d: Passivation of metal alloys is an important phenomenon that enables the widespread use of metallic materials in modern society. The electrochemical APXPS (EC-APXPS) setup is well-suited for studies of the formation and breakthrough of passive films under real-life conditions, i.e., in the presence of electrolyte under electrochemical control. Thus, using *in situ* APXPS, it was shown that in a NaCl electrolyte under anodic potential, the native oxide of Ni-Cr-Mo alloy (rich in Cr^{3+}) doubles in thickness and becomes enriched with Mo^{6+}.

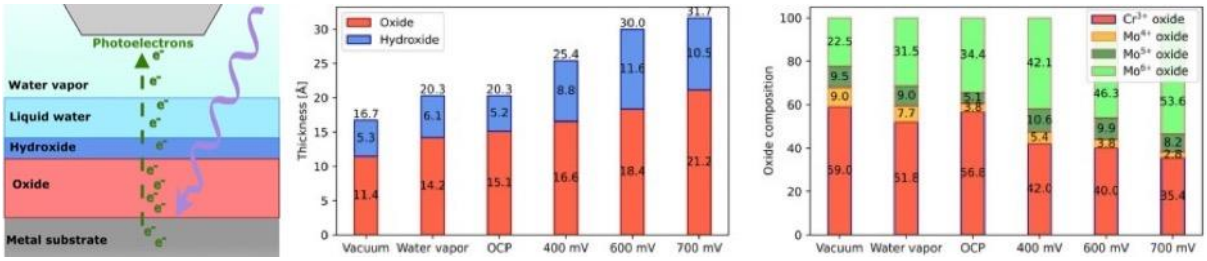

Figure 3.3. (Left) Layered model of passive film illustrating the metal substrate, oxide layer, hydroxide layer, liquid water layer, and the surrounding water vapor. (Middle) Oxide and hydroxide thickness for different exposure conditions. (Right) Total oxide composition for various exposure conditions (Larsson *et al., 2022).*

Examples of work: Larsson *et al., 2022.*

Ongoing developments: Dedicated experimental platform for battery and corrosion research using APXPS at the HIPPIE beamline.

Potential Developments: Electrochemical Scanning Photoemission Microscope for *operando* and *in situ* APXPS at the solid–liquid interface with high spatial resolution.

AP: 3 iv | b, c, d: The Atomic Layer Deposition (ALD) process is one of the backbones of today's electronic device fabrication. A critical property of ALD – the layer-by-layer growth rate – can differ

significantly depending on multiple experimental parameters. In contrast to typical constant growth rates under steady-state conditions usually reached after hundreds of ALD cycles, the deposition at the early stages does not follow the same kinetics or chemistry. At SPECIES, a unique dedicated ambient pressure cell for ALD research can be used to study the ALD process *in situ* during these initial stages. Thus, it was observed that contrary to the commonly accepted model, formation of HfO_2 could be directly initiated on InAs irrespectively from the presence or the nature of the oxide or hydroxyl groups (D'Acunto *et al.,* 2020; Kokkonen *et al.,* 2022, D'Acunto *et al., 2022*).

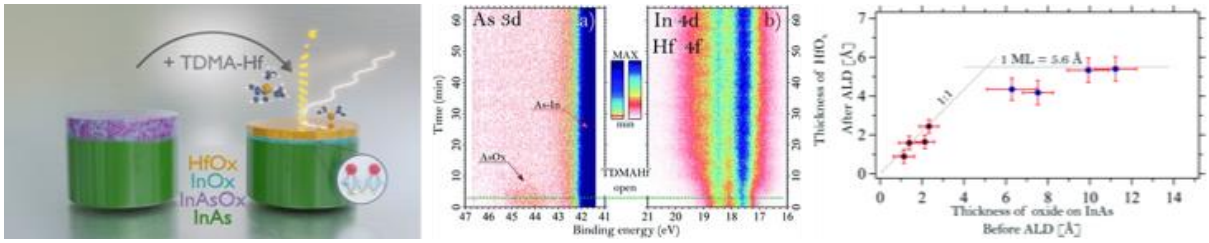

Figure 3.4. (Left) The first step in ALD of HfO_x (high-k oxide) on an InAs substrate (III–V semiconductor), highlighting the removal of the native $InAsO_x$ layer. (Middle) Series of (a) As 3d and (b) In 4d/Hf 4f ambient pressure XP spectra measured during the first half-cycle of ALD. (Right) Correlation graph between the oxide thickness of InAs before the deposition and the thickness of the HfO_x layer after the first half cycle (D'Acunto *et al.,* 2022).

Examples of work: D'Acunto *et al.,* 2020; Kokkonen *et al.,* 2022; D'Acunto *et al.,* 2022

Ongoing developments: Dedicated sample environment for ALD research and its continuous improvement and adding new capabilities.

AP 4: i, iv | c: Thermal catalysis is at the center of the circular economy, playing a vital role in manufacturing chemicals and energy distribution. *In situ* and *operando* APXPS is an essential technique for studying elementary processes occurring at the surface of the active material in the presence of reagents. With the dedicated catalysis sample environments (cells), HIPPIE and SPECIES-APXPS beamlines are well-equipped to perform research within the model and applied catalysis fields. Multiple industry-relevant catalytic processes and model systems have been successfully investigated using the help of the HIPPIE and SPECIES-APXPS instruments.

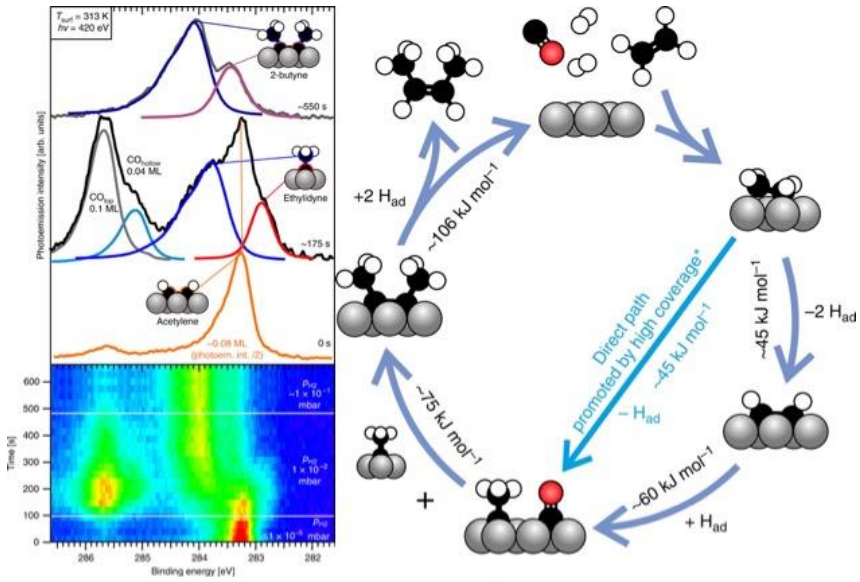

Figure 3.5. (Left) C 1s spectra were recorded during exposure of an acetylene-covered Co(0001) surface to increasingly high H_2 pressures. Note that the CO signal at 285.8 eV appears on the surface while dosing H_2. (Right) Proposed catalytic cycle of CO-induced ethylene dimerization based on the measurements from the HIPPIE beamline (Weststrate *et al.,* 2020).

Examples of work: Divins *et al.,* 2021; Weststrate *et al.,* 2020; Patera *et al.,* 2022.

Recently, a novel time-resolved pump-probe (event-averaged) APXPS setup using chemical perturbations (gas pulses) has been successfully implemented at the HIPPIE and SPECIES-APXPS beamlines allowing *operando* spectroscopy down to microsecond time resolution. This method enables observing catalytic reactions in real-time with unprecedented details.

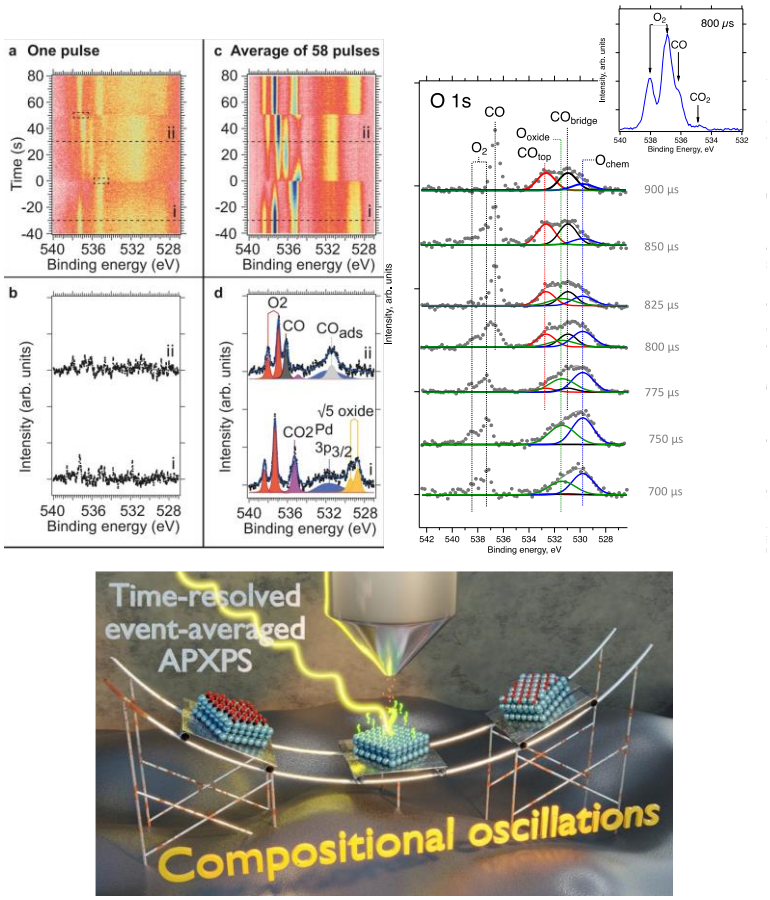

Figure 3.6. (Top a, c) Image plots of time-resolved O 1s data acquired before and after event-averaging 58 pulses. (Top b, d) Single spectra recorded along the dotted lines i and ii in panels (a and c) and the curve fitting and peak assignment for the event-averaged data (Knudsen *et al.,* 2021). (Top right) The time-resolved O 1s spectra were measured across the rising edge of pressure pulse of CO into the flow of O_2 on Pt(111) surfaces. The inset shows the gas-phase spectra corresponding to the time delay with the highest reactivity (highest CO_2 production). (Bottom) Artistic interpretation of the time-resolved pump-probe technique using chemical perturbations (composition oscillations).

Examples of work: Event-averaged time-resolved APXPS: Knudsen *et al.,* 2021, Boix *et al.,* 2022, Shavorskiy *et al.*, 2021.

Potential developments: Dedicated sample environment for sub-millisecond event-averaged time-resolved APXPS including fast detector.

AP 5: ii | c: Electrocatalysis is a process important for e.g. the CO_2 reduction reaction (RR), the production of green hydrogen via water electrolysis, and novel efficient ways of producing ammonia. Using o*perando* APXPS, researchers can observe changes in the chemical composition at the interface between the electrocatalyst and electrolyte during the electrochemical reaction. Thus, researchers have recently used the electrochemical setup at HIPPIE to study the evolution of Cu-based model electrocatalyst for CO_2RR under reaction conditions. The data have clearly shown the Cu active centres being in the metallic state, helping to resolve a long-standing debate about the role of oxygen species in reducing CO_2.

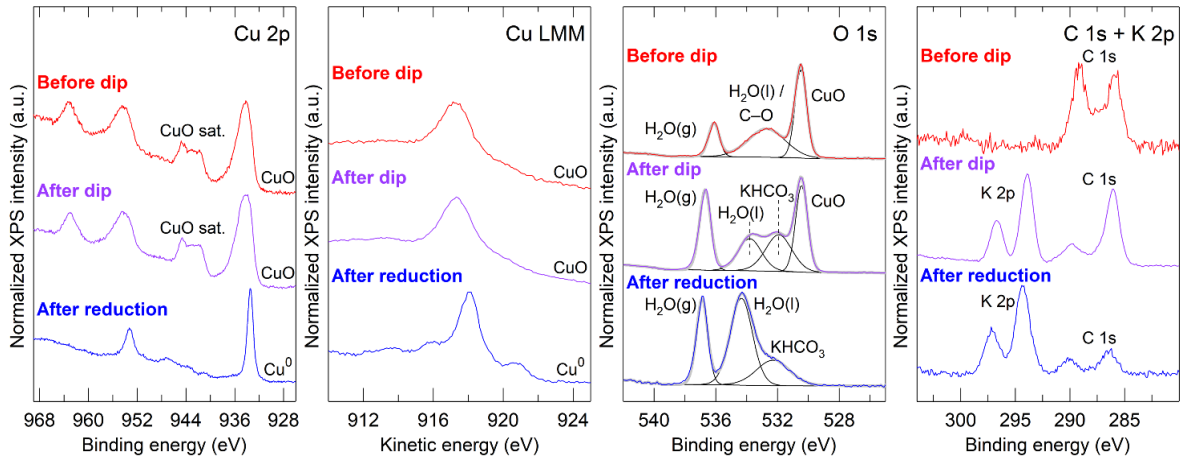

Figure 3.7. Oxide-derived ALD Cu electrocatalyst for CO_2RR analysed in situ by EC-APXPS. XPS spectra were recorded before dip into, after dip, and after electrochemical reduction under gas evolution conditions. Cu 2p3/2 and Cu LMM spectra show evidence of complete reduction of CuO to metallic Cu (Ali-Löytty et al. 2022).

Ongoing development: Dedicated experimental platform for electrocatalysis research using APXPS at the HIPPIE beamline.

Potential development: Quick *operando* XAS.

AP 6: iii | c, d: Atmospheric and environmental chemistry processes can be studied using APXPS at both SPECIES and HIPPIE. Recently the chemistry of salt aerosols has been studied during their interaction with water vapour. Such interactions play a crucial role in multiple critical processes in the atmospheres of the Earth and Mars. APXPS and APXAS at HIPPIE were used to investigate Martian salt analogues sampled from the Qaidam Basin, a terrestrial analogue for Mars. Surfaces of such salt analogues are susceptible to gas-phase water, i.e., the surface gets fully solvated at RH = 5%.

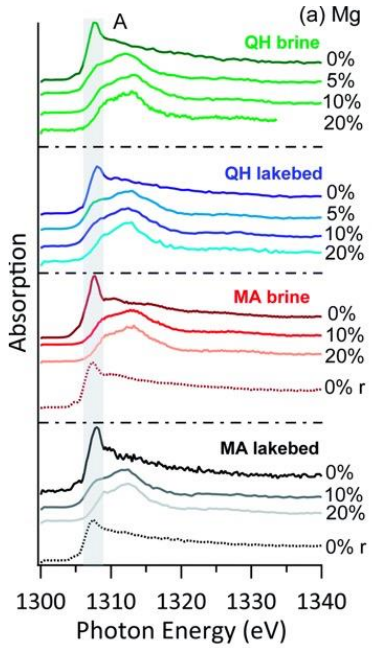

Figure 3.8. NEXAFS of Mg K-edge of the brine and lakebed samples at various relative humidity (Kong *et al.,* 2022).

Examples of work: Kong *et al.,* 2022; Lin *et al.,* 2021.

Potential developments: (1) Dedicated sample environment for highly controlled temperatures. (2) Upgrade of the gas introduction system to more accurately dose known mixtures with high level of automation.

AP 7: i | d: Perovskite solar cells are promising as lightweight, thin-film devices with low processing costs. In past years their efficiency started rivalling that of crystalline silicon cells, and there are concentrated efforts in commercializing them. Finding efficient, stable, and affordable electrode materials is one of the key steps toward using perovskite cells in everyday applications. Recently a promising low-cost electrode material based on metallic Copper was tested at SPECIES against degradation by oxygen and moisture. It was shown that in addition to the expected CuI, which is expected to have a passivation effect on the film, large quantities of several new copper salts were observed at the electrode/perovskite interface. This information has direct implications for the design of the current collectors for these novel PV materials.

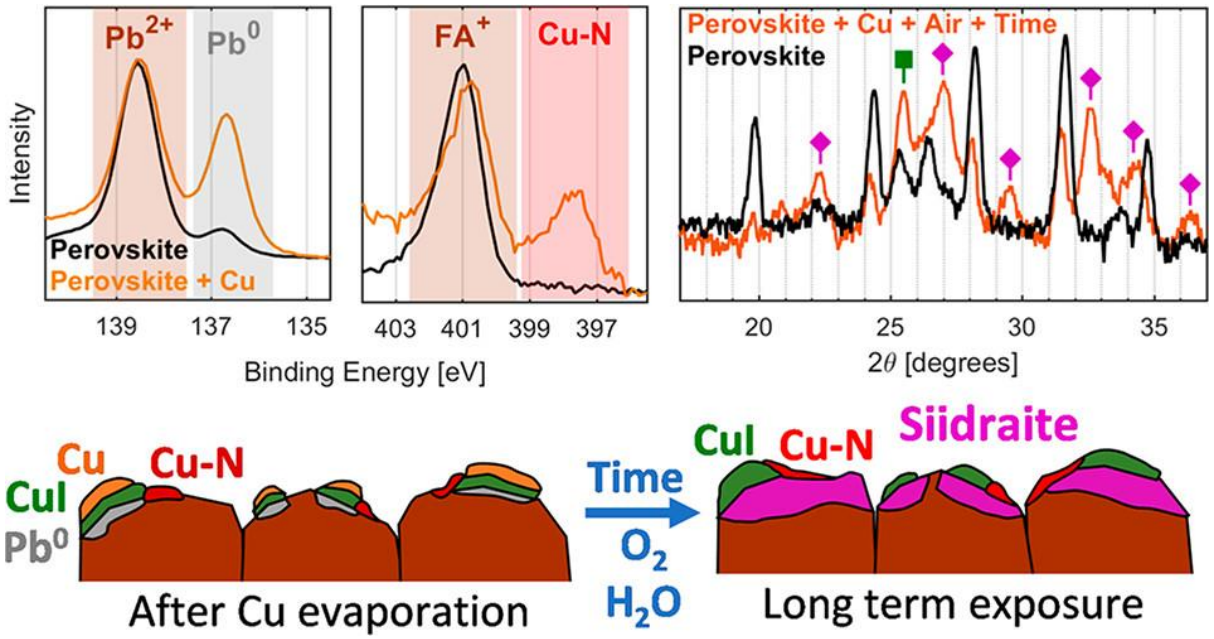

Figure 3.9. (Top left) Photoelectron spectra from $Cs_{0.17}FA_{0.83}PbI_3$ before and after evaporation of Cu. (Top right) X-ray diffractograms of thin film samples with and without Cu. (Bottom) Schematic illustration showing the different treatments and their impact on the structure of the $Cs_{0.17}FA_{0.83}PbI_3$/copper interface (Svanström *et al.,* 2022).

Examples of work: Svanström *et al.,* 2022.

Potential developments: (1) Dedicated sample environment for high-temperature studies. (2) An upgrade of the gas dosing system for more accurate control of gas mixtures. (3) An upgrade of the SPECIES beamline capabilities with a new grating.

AP 8: iv | d: 2D materials (e.g., Graphene, h-BN, MXenes) are a fascinating class of materials whose unique properties arise from their low dimensionality. For example, an improvement in the catalytic properties of multiple surfaces covered by graphene (space-confined catalysis) has been reported. The APXPS and time-resolved APXPS at HIPPIE and SPECIES beamlines have been extensively used to study the thermodynamics and kinetics of various surface processes in the presence of 2D materials. For

example, it was demonstrated that the presence of h-BN or Graphene successfully hinders the oxidation of a Cu surface up to 120 °C, although via different mechanisms.

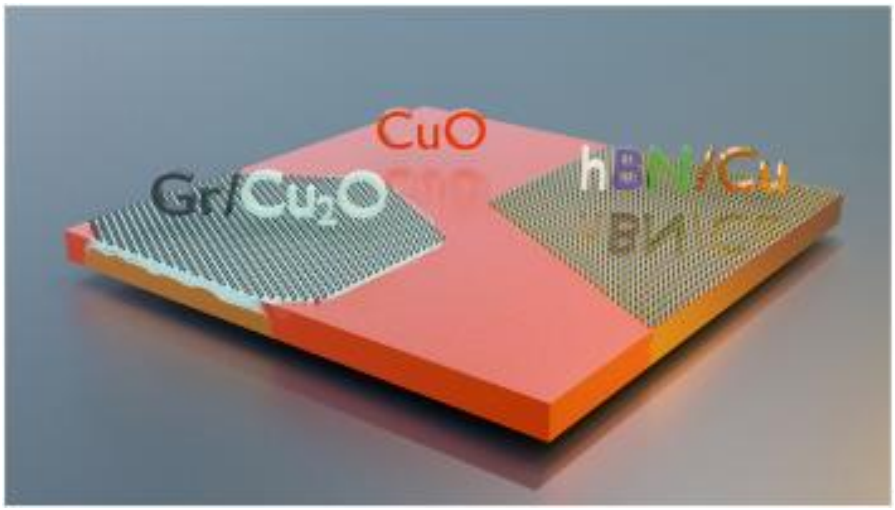

Figure 3.10. Mechanisms of protection of copper by Graphene and h-BN (Scardamaglia et al., 2021).

Examples of work: Boix *et al.,* 2022 ; Näslund *et al.,* 2021; Scardamaglia *et al*., 2021.

Potential developments: Dedicated sample environment for sub-millisecond event-averaged time-resolved APXPS including a fast detector.

AP 9: ii | b, c: Steel is an integral part of modern society and its manufacturing industry is continually interested in reducing the harmful emissions from the processing while making the products more durable. The steel industry is highly dependent on fossil fuels and contributes a significant amount to global CO_2 emissions. A suggested pathway for improving the manufacturing processes is to use hydrogen in the process of product manufacturing. However, very little information or experimental studies currently exist on the related surface reactions on a molecular level. The dedicated sample environments provided at the HIPPIE and SPECIES-APXPS beamlines provide an especially convenient place to conduct experiments to fill the knowledge gap in these industrial processes. The behavior of steel alloys at high temperatures under ambient conditions is an important area of study where the Ambient Pressure XPS will make a significant impact.

Potential developments: Dedicated sample environment for high-temperature studies and clean environments.

3.2 FlexPES

The FlexPES beamline caters to the experimental needs of the materials science community, offering the possibility to perform a variety of photoemission and soft X-ray absorption experiments in the photon energy range of 40 – 1500 eV. The double-striped toroidal refocusing mirrors ensure maximum flexibility – up to four endstations can be accommodated on the two branches of the beamline simultaneously, and each of these endstations can take advantage of different focusing conditions. The endstations offer a diverse range of experimental techniques, detectors, and sample handling facilities and can be used with a variety of sample delivery systems. Both hard and soft (liquids, gases) matter can be studied at FlexPES solid-state and liquid endstation as well as with the ICE setup.

Specific examples of different research areas are given in the following:

FP 1: i | c: A large variety of applications of solar-powered devices calls for diversity in the light-harvesting materials used in them. Materials used in indoor solar cells or self-powered wearable devices differ from those used in rooftop modules. Selection of the suitable material for the proper purpose relies on the readily available catalogues of photovoltaic materials, which describe the multitude of their physical and chemical properties as well as quantum efficiency and cost. UHV XPS and XAS available at FlexPES are the key techniques to obtain such characteristics by measuring the chemical composition and electronic structure of the PV materials and their bonding interactions with the supporting surfaces.

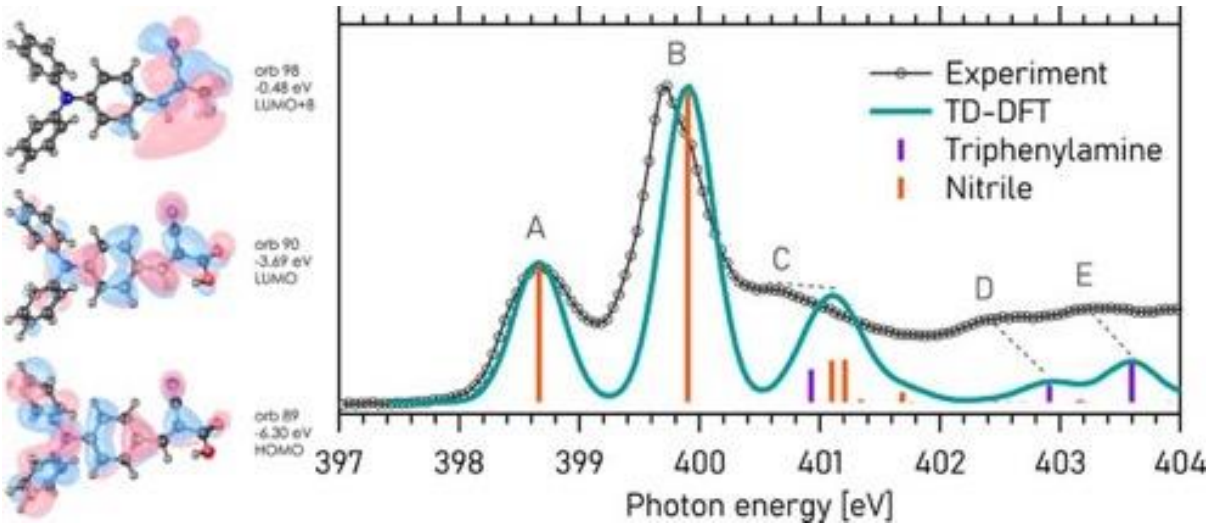

Figure 3.11. (Left) Selected ground state molecular orbitals obtained from DFT. (Right) Comparison between experimental NEXAFS and that simulated with TD-DFT (Temperton *et al.,* 2021).

Examples of work: Temperton *et al.,* 2021.

Potential development: (1) High throughput soft X-ray XAS setup. (2) Ambient pressure analyser for studies of liquid and gaseous samples.

FP 2: iv | c, d: New metallic alloys (e.g., Ni-superalloys) found widespread use in applications with harsh conditions, such as nuclear power plants, gas turbines, and oil and gas wells due to their excellent mechanical properties. However, the corrosion properties of these new materials, such as the thickness of the passive film and composition of the native oxide, are still not well understood. By varying the surface sensitivity in the XPS measurement, it is possible to perform a non-destructive and chemically specific in-depth characterization of the passive film formed on such Ni superalloys.

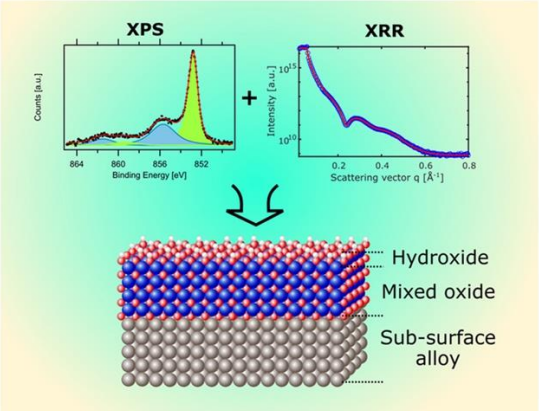

Figure 3.12. A combination of photoemission, x-ray reflectivity measurements, and DFT calculations reveal the structure of the native oxide layer on a Ni superalloy (Larsson *et al.,* 2022).

Examples of work: Larsson *et al.,* 2022.

FP 3: iv | c, d: Unique properties of the novel layered materials for nanoelectronic devices often arise from the interface between different layers. XPS with varying surface sensitivity is an ideal technique for studying the properties of these interfaces and their evolution during preparation. For example, researchers have performed spectroscopic characterization of the interface oxide between III–V nanowires and high-k dielectrics for combining transistors and resistive memory units. These findings have helped to find conditions for growing a thick interfacial oxide layer, which helps this interface to serve both as a transistor selector and a high-performance resistive memory unit.

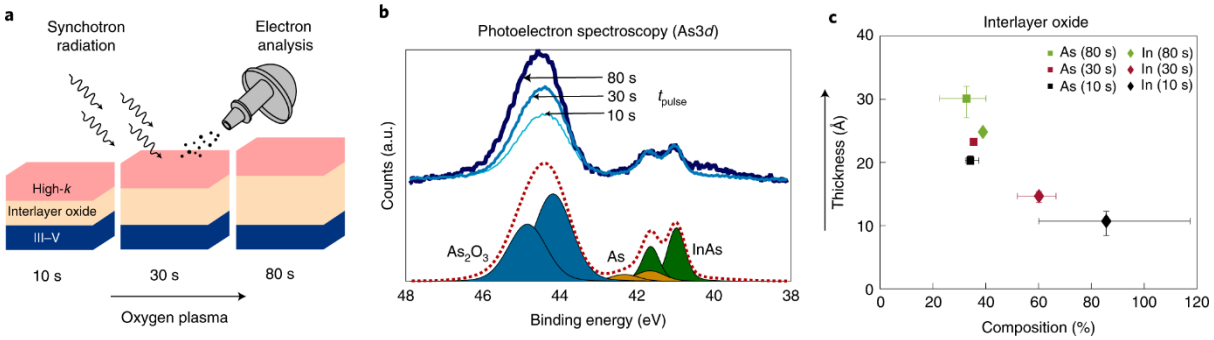

Figure 3.13. Schematic of planar RRAM structures which, on the PEALD of HfO_2 (pink colour), feature a plasma-dependent interlayer oxide growth (tan colour) on the III–V substrate (blue colour). **b**, As3*d* photoelectron spectra depict the increase in arsenic oxide concomitant with t_{plasma} (top) and, for example, deconvolution (bottom). **c**, Thickness and compositional changes in the III–V/high-k interlayer expressed as a percentage of volume; arsenic and indium oxides are represented as squares and diamonds, respectively (Saketh *et al.,* 2021).

Examples of work: Saketh *et al.,* 2021.

FP 4: iii | c, d: The chemical reactions occurring at the interface of liquid water and air play an important role in processes in Earth's atmosphere and hence impact the planet's environment and climate. It is, therefore, of high use to understand on the basic level the chemistries of these reactions and their kinetics. The liquid jet setups available at FlexPES and HIPPIE photoemission beamlines and Veritas RIXS beamline can be used to measure such processes under natural conditions. For example, recent measurements of the molecular properties of the surface of ethanol–water mixtures revealed a rapid non-linear increase in the surface ethanol concentration for mixtures with below 0.1 molar

fraction of ethanol. At this point, the ethanol molecules form a well-ordered monolayer with 40° tilt angle (with FWHM of the distribution below 20°). At fractions above 0.1, the surface concentration of ethanol remains constant, but the tilt angle of the molecules gradually increases to 55° (FWHM of the distribution is 60°), indicating disorder.

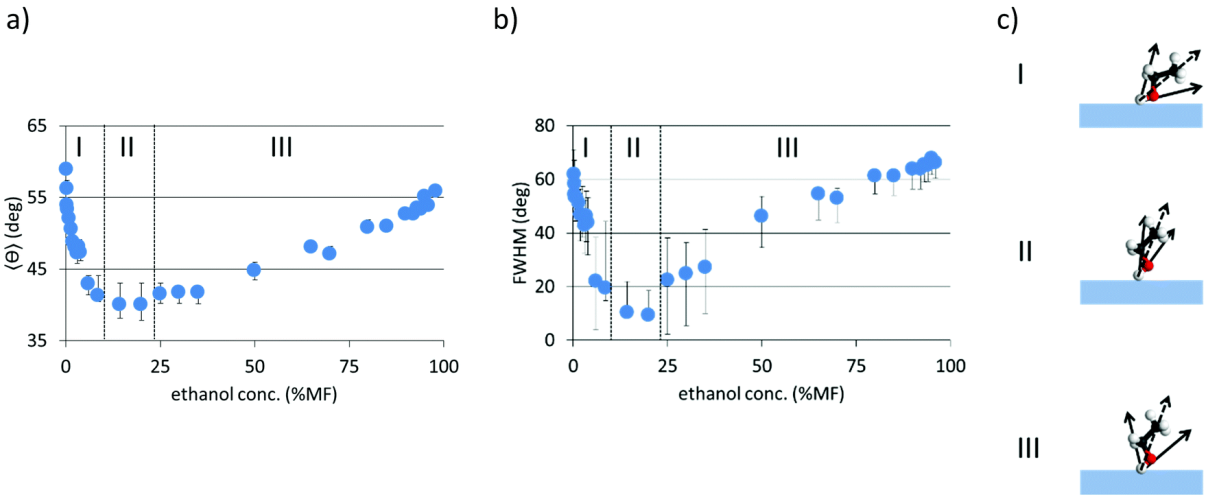

Figure 3.14. (a) The average polar orientation angle $\langle\vartheta\rangle$ and (b) full-width-at-half-maximum of the orientational distribution of EtOH molecules in water–ethanol solution. (c) Schematic representation of the resulting fitted orientation and width of the angular distribution in the three different concentration regions that were defined (Kirschner *et al.,* 2021).

Examples of work: Kirschner *et al.,* 2021.

Potential development: Ambient pressure analyser for studies of liquid and gaseous samples.

3.3 Bloch

The Bloch beamline is dedicated to high-resolution angle-resolved photoelectron spectroscopy (ARPES) for studying the electronic structure of surfaces and 2D materials. Both linearly and circularly polarized light can be provided. The unique property of the beamline is a beam size down to 10µm x 10µm which allows measuring the electronic structure of small surface domains. In addition, the beamline has a high-performance hemispherical electron energy analyser with an electronic deflection mode, enabling Fermi surface mapping without needing to rotate the sample. Combining the analyser and the small spot size is highly advantageous for studying small or inhomogeneous samples.

Specific examples of different research areas are given in the following:

BL 1: i | d: Bloch can play a major part in the ongoing efforts to understand high-temperature (HT) superconductivity, which would completely revolutionize clean energy distribution. Large classes of strongly correlated systems (e.g., heavy fermion – HF – materials) exhibit properties of quantum criticality and unconventional superconductivity. Understanding the properties of such materials at low temperatures is an important step toward harnessing HT superconductivity. A significant problem in studying such systems is preparing a sample with a large single crystal domain (hundreds of micrometres in size) required for performing high-quality ARPES. However, many of these materials cannot be cleaved predictably, leaving samples with domains of only a few tens of micrometres. The small spot at the Bloch beamline is a unique characteristic allowing us to successfully obtain excellent-quality data from the tiny individual domains.

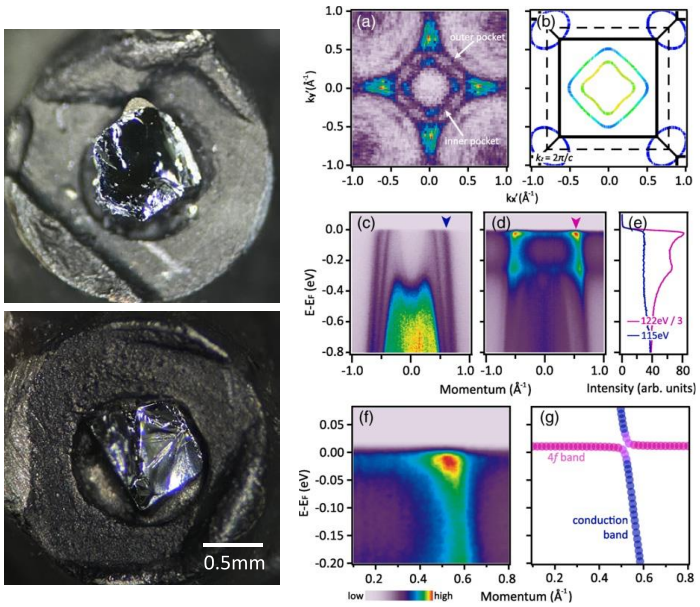

Figure 3.15. (Left) images of two cleaved (001) samples showing flat areas used for ARPES measurements. (Right) 4f contribution to pockets near bulk Z point (Wu *et al*., 2021).

Examples of work: Wu *et al*., 2021.

Ongoing development: Low-temperature manipulator allowing <10 K measurements.

BL 2: iv | d: Quantum materials, such as spintronic and topological materials, offer new possibilities for devices, enabling, for example, lower energy computation or novel thermoelectric generation. ARPES is typically a key tool to understand the unique electronic properties of these materials, which are being leveraged in the novel devices.

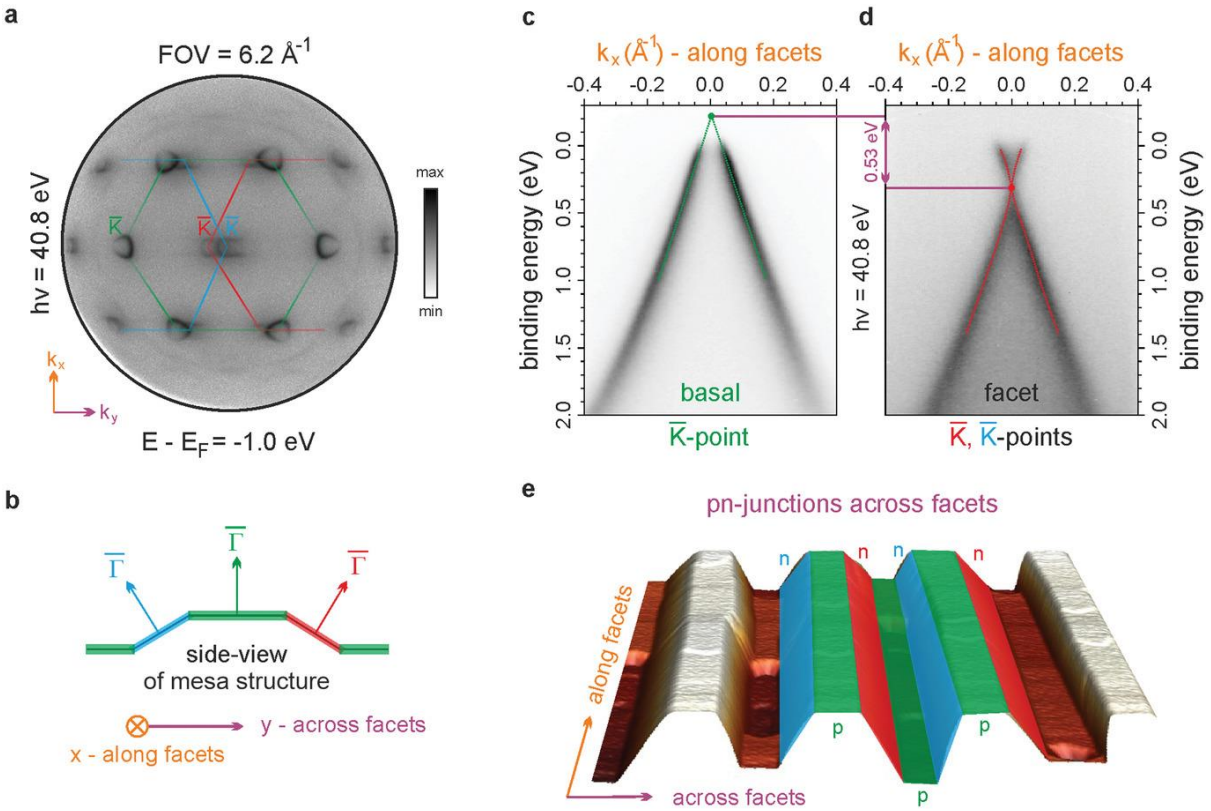

Figure 3.16. Periodic nanoarray of graphene pn-junctions across the facets. a) ARPES constant-energy cut taken 1.0 eV below the Fermi level. b) Schematic side view of the mesa structure. c,d) ARPES energy–momentum cuts acquired at the K̄-points of c) basal and d) facet Quasi-free-standing monolayer graphene (QFMLG), respectively. e) The coloured regions superimposed on top of the 3D AFM image show the spatial distribution of basal (green) and facet (red/blue) QFMLG over the SiC mesa structures (Karakachian *et al.*, 2022).

Examples of work: Karakachian *et al.*, 2022; Pan *et al.*, 2022.

Potential developments: <10 K cryo manipulator at the Spin-resolved endstation. .

3.4 Balder

The Balder beamline has capabilities for both spectroscopy and scattering and diffraction. For simplicity and due to the interconnected research, all Balder activities in this document are gathered under Scattering and Diffraction, see section 2.1.

4. Imaging

MAX IV provides a suite of beamlines offering a range of different imaging capabilities, with techniques that enable structure determination of a sample with high resolution, both at the sample surface and within the bulk of a sample in three dimensions. The relevant beamlines (and techniques) for imaging are MAXPEEM (spectroscopic photoelectron and low energy electron microscopy), NanoMAX (scanning X-ray diffraction imaging, coherent diffraction imaging / ptychography), SoftiMAX (scanning transmission X-ray microscopy, ptychography), ForMAX (X-ray microtomography, scanning SWAXS imaging) and DanMAX (X-ray microtomography, X-ray diffraction computed tomography). These beamlines enable materials characterization within the following research areas relating to WISE related activities:

- Structures: When coupled with tomography acquisition and reconstruction, features coming online this year at ForMAX and DanMAX, X-ray imaging provides the capability to visualize the structure of a sample virtually, non-destructively, and in three dimensions. Furthermore, phase contrast methods allow small changes in sample density to be measured, allowing soft materials, such as polymer materials at interfaces, to be imaged. Imaging techniques such as STXM at SoftiMAX enable access to absorption edges that give chemical contrast without the need for labelling or staining methods, while X-ray fluorescence imaging allows elemental mapping with high sensitivity. Imaging methods that exploit coherent X-rays, such as those available at NanoMAX, enable recovery of the complex amplitude scattered by a sample, where the resolution achievable using coherent diffraction imaging methods is currently around 10 nm.
- Properties: 4D imaging – 3D + time – provides the ability to follow temporal changes in the sample microstructure using tomographic imaging, *in situ* during application of e.g. external heat or pressure. This offers important information about the link between micro- and nano-scale structure and material properties (structure–function relationship). Exploiting X-ray diffraction and scattering contrast in imaging provides unique insights into the levels of order and disorder in matter, such as in the mapping of defects and strain.

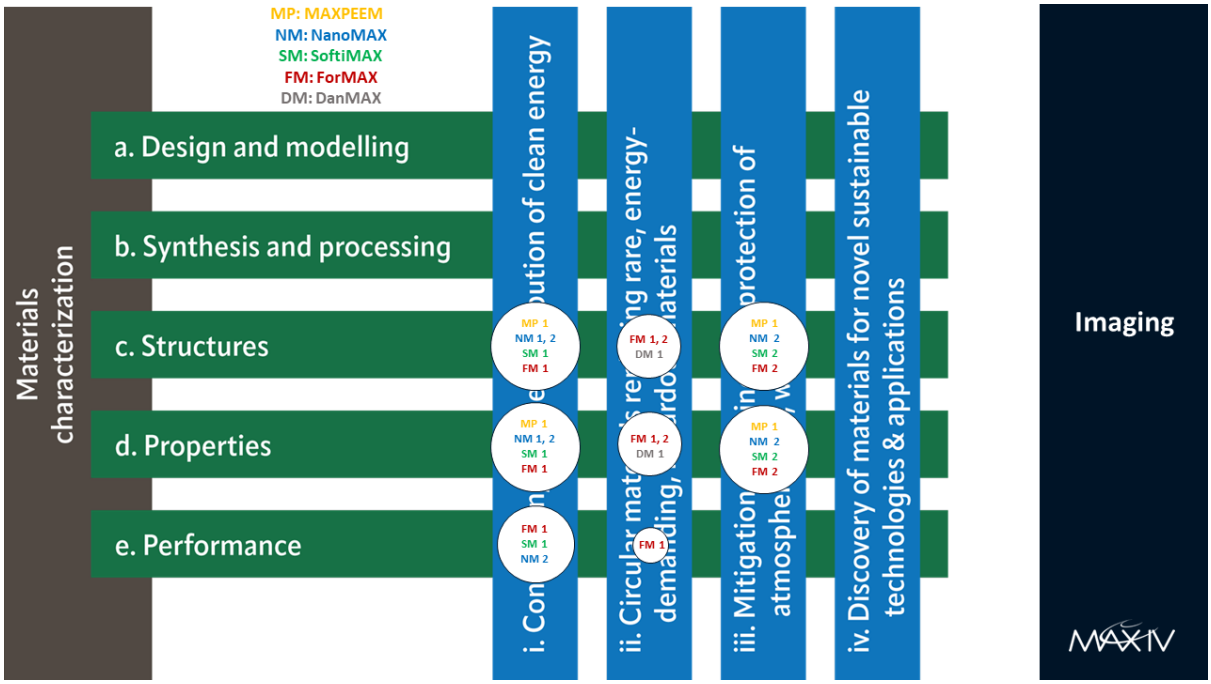

Figure 4.1. The WISE matrix of research areas, with specific examples from the imaging beamlines shown and labelled.

4.1 MAXPEEM

The MAXPEEM beamline provides surface imaging techniques with structural, chemical, electronic, and magnetic contrasts at spatial resolutions in the nanometre range. Spectroscopic photoelectron and low energy electron microscopy (SPELEEM) provides easy access to all of these contrast mechanisms in a single instrument. This enables research in a wide range of disciplines – materials science, nano-science, heterogeneous catalysis, corrosion science, and polymer science, to name but a few. SPELEEM also has the advantage of having a large dynamic range of fields of view of up to ~100 µm thereby facilitating easy access to not only nanometre, but also micrometre, scale structure. As the detection in SPELEEM is done at video rates, monitoring of real-time dynamical processes is possible.

MP 1: i | c, d & iii | c, d: Engineering tunable graphene−semiconductor interfaces while simultaneously preserving the superior properties of graphene is critical to graphene-based devices for electronic, optoelectronic, biomedical, and photo-electrochemical applications. At MAXPEEM, researchers can study two-dimensional surfaces and interfaces with a combination of techniques. An example is the study of separation and transport of charges in a graphene/cubic silicon carbide Schottky junction (Li *et al.,* 2020).

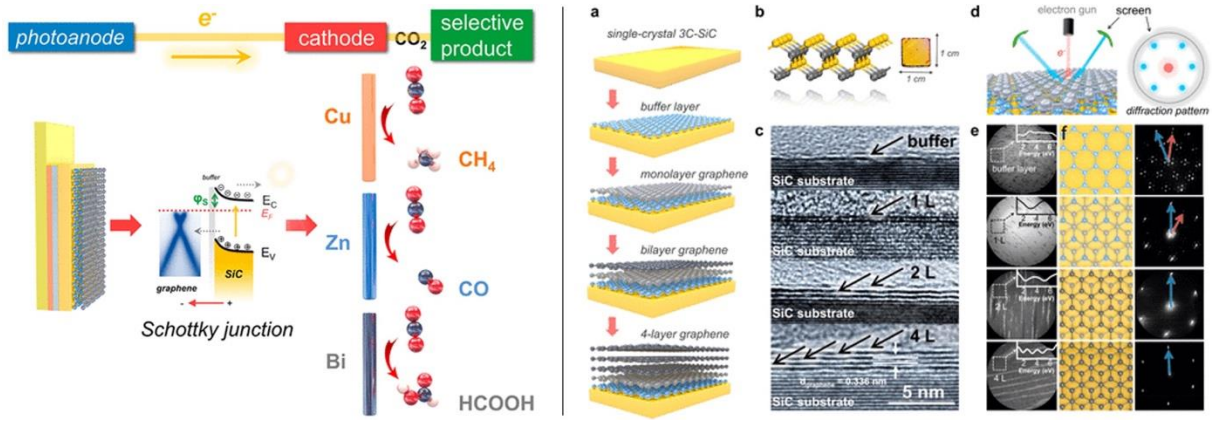

Figure 4.2. (Left) Visualization of the electronic structure of a graphene/cubic SiC Schottky junction. (Right) Synthesis and characterization of graphene/3C-SiC samples, including (e) low-energy electron microscopy (field of view = 5 µm) and (f) low-energy electron diffraction images of the as-grown samples (Li *et al.,* 2020).

4.2 NanoMAX

NanoMAX, the hard X-ray nanoprobe beamline, comprises two endstations and accommodates multiple imaging and scattering methods. The methods are either based on coherence to achieve spatial resolution, such as in ptychography or coherent diffraction imaging (CDI), or on the focused beam such as in scanning diffraction or X-ray fluorescence (XRF) mapping experiments. The diffraction endstation exploits intense coherent photon flux using KB mirrors for focusing to 40–200 nm, enabling methods such as CDI in forward and Bragg geometries, nano-diffraction in both geometries, and 2D XRF and X-ray absorption near-edge structure spectroscopy (XANES) imaging. The tomography endstation, based on Fresnel zone plate (FZP) optics, is optimized to provide 10–50 nm spatial resolution for 2D and 3D tomographic experiments with XRF, XANES contrast, and CDI as the primary imaging methods.

NM 1: i |c, d: The interest in metal halide perovskites has grown as impressive results have been shown for solar cells, light emitting devices, and scintillators, but this class of materials has a complex crystal structure that is only partially understood. In particular, the dynamics of the nanoscale ferroelastic domains in metal halide perovskites remains difficult to study. An ideal *in situ* imaging method for ferroelastic domains requires a challenging combination of high spatial resolution and long penetration depth. NanoMAX has the ability to retrieve local structural properties at varying temperatures, by using a 60 nm X-ray beam, which was demonstrated for a single-crystal perovskite nanowire (Marçal *et al.,* 2020).

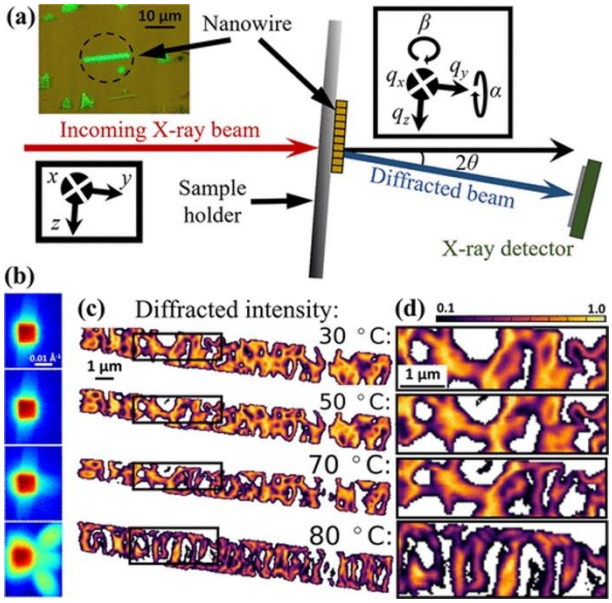

Figure 4.3. Scanning X-ray diffraction imaging of a single perovskite nanowire as a function of temperature, including: (a) schematic representation of the experimental setup; (c-d) Real-space maps showing local diffracted intensity (Marçal *et al.,* 2020).

Axially heterostructured nanowires are a promising platform for next generation electronic and optoelectronic devices. Reports suggest a more complex strain distribution and increased critical layer thicknesses than in thin films, but mapping the strain inside a single nanowire is challenging. NanoMAX can perform this type of measurement using scanning X-ray diffraction with a nanofocused X-ray beam, and users have demonstrated this ability for an InP/GaInP nanowire (Hammarberg *et al.,* 2020).

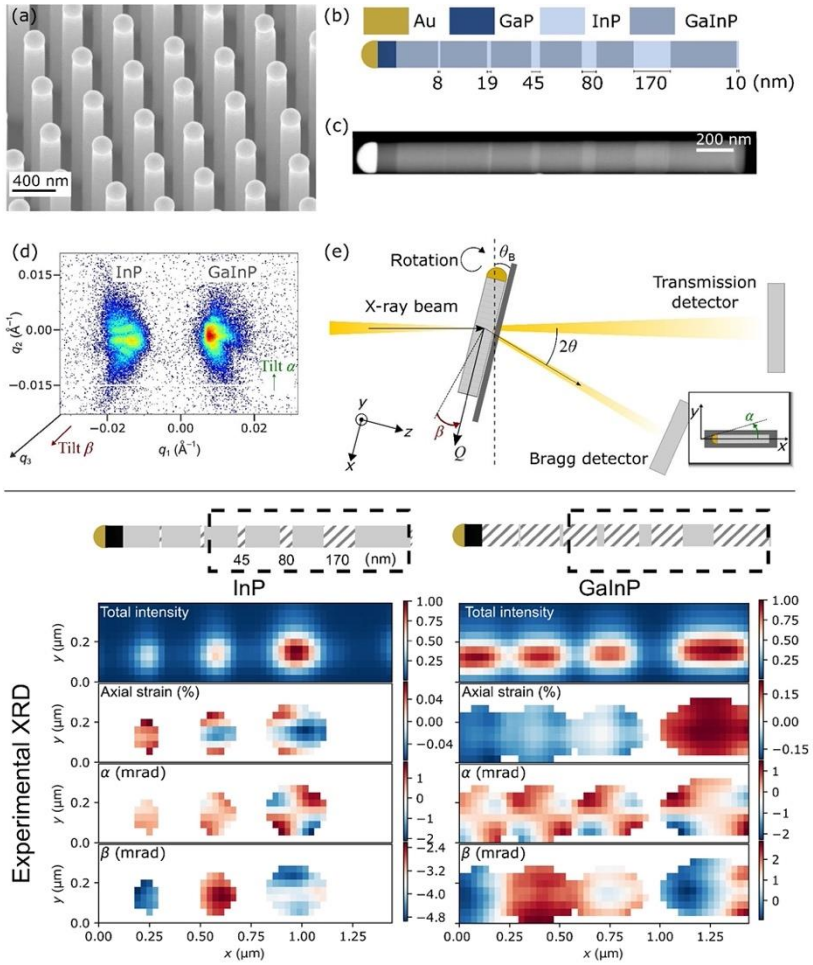

Figure 4.4. Schematic (d-e) of the scanning X-ray diffraction measurement of a single nanowire (a-c). Below, the strain distribution in a single heterostructured nanowire, with pixel sizes of 30 and 40 nm in *x* and *y*, respectively (Hammarberg *et al.,* 2020).

NM 2: i | c, d & iii | c, d: Monitoring the development of hierarchical pore structure in heterogeneous catalysts is important for understanding transport phenomena during chemical reactions. 2D X-ray ptychography and 3D ptychographic X-ray computed tomography (PXCT) enable to understand complex synthesis pathways of porous materials. For example, measurements performed at the cSAXS beamline of the Swiss Light Source provided quantitative information on pore structure, size, and shape in Ni/Al_2O_3 catalysts with connected meso- and macropore networks, with 3D spatial resolution approaching 50 nm (Weber *et al*., 2022).

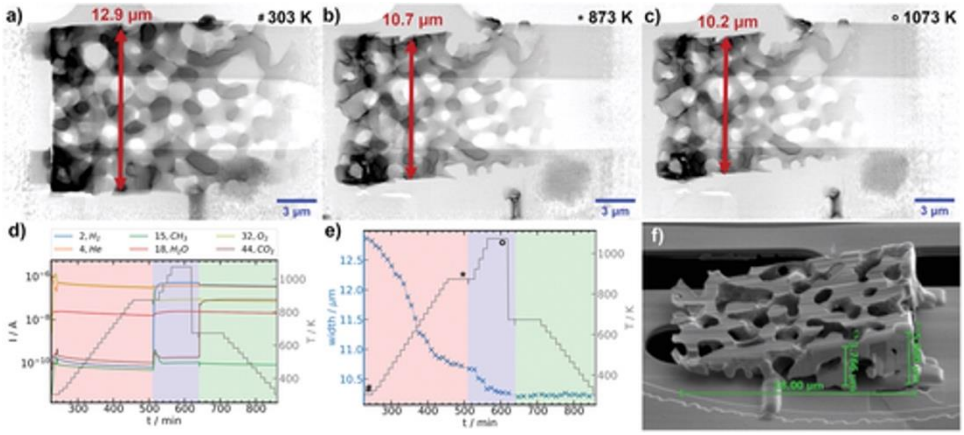

Figure 4.5. *In situ* 2D X-ray ptychography of a dried gel Ni/Al_2O_3 catalyst sample in a nanoreactor setup: a) initial state of the dried gel; b) after calcination at 873 K; (c) after activation at 1073 K (Weber *et al*., 2022).

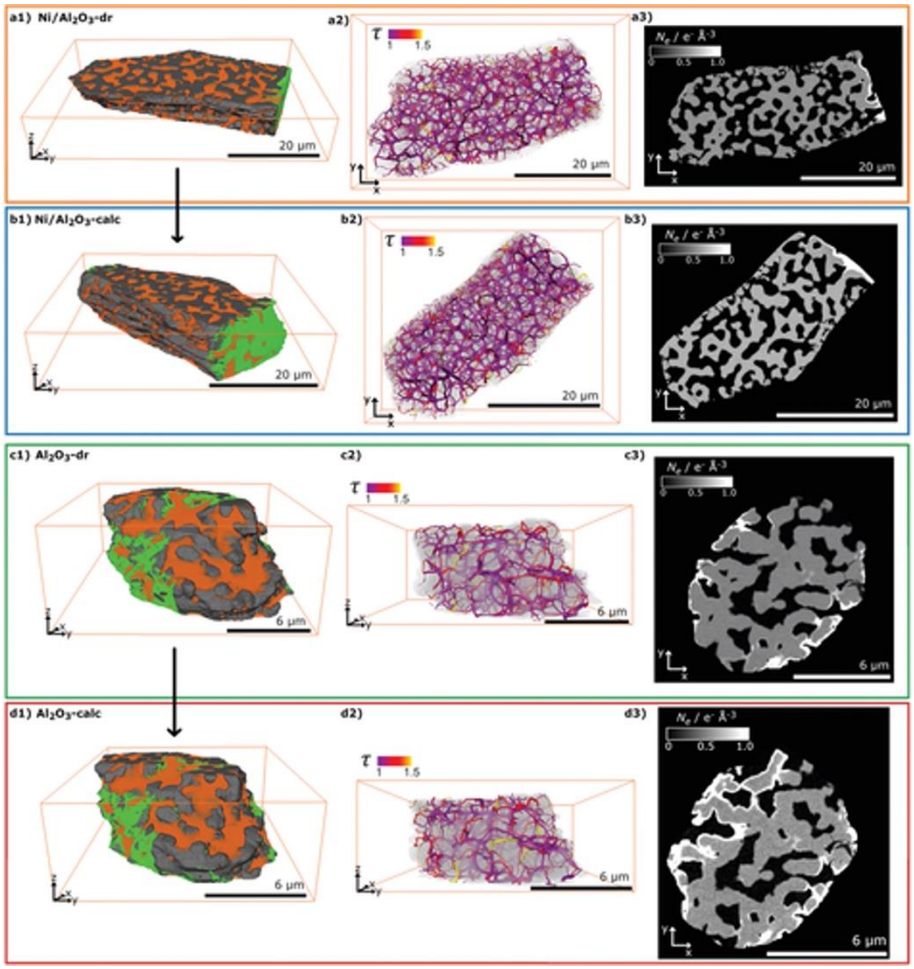

Figure 4.6. 3D ptychographic tomography measurements of a Ni/Al_2O_3 catalyst sample: PXCT volume renderings (left), pore network models derived from PXCT data (middle), and greyscale slices (Weber *et al*., 2022).

The first commissioning PXCT measurements performed at the NanoMAX beamline have achieved a resolution of approximately 80 nm (Kahnt *et al*., 2020).

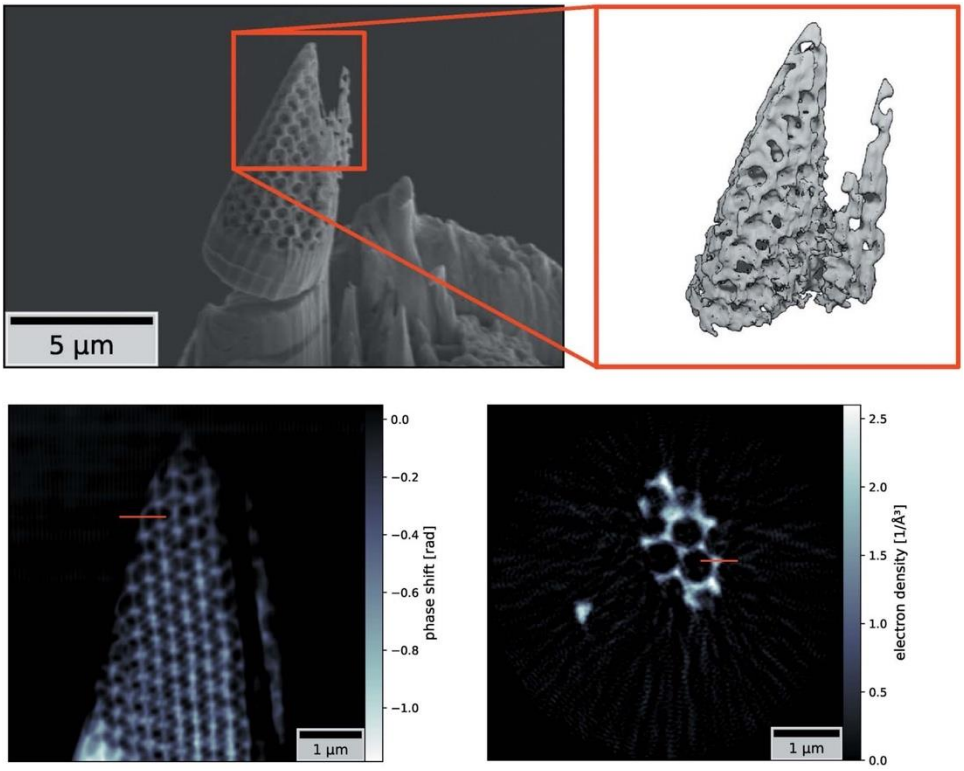

Figure 4.7. Top: 3D rendering of the reconstructed electron density in a nickel-based inverse opal sample obtained from PXCT measurements. Below: (left) phase image of a ptychographically reconstructed projection; (right) tomographic slice through the reconstructed electron density volume (Kahnt *et al*., 2020).

4.3 SoftiMAX

SoftiMAX is a soft X-ray beamline dedicated to spectromicroscopy and coherent imaging. The beamline will have two branch lines: one branch (now available) for STXM and ptychography with a sub-100 nm focus, and one modular line for coherent techniques that require a larger beam size. STXM offers chemical specific information on nm-size areas of a thin sample (typically 100 nm to 1 µm), at absorption edges between photon energies 275 eV and 1600 eV and with spatial resolution between 20-60 nm (depending on energy range).

SM 1: i | c, d, e: Fuel cells can play a key role in green energy, but still face technological challenges that are limiting widespread applications. Using scanning transmission X-ray microscopy (STXM) and ptychography, it is possible to study the interfaces inside fuel-cell catalyst layers. For example, the interface between perfluorosulfonic acid (PFSA) polymer electrolytes and Pt nanoparticles in a model hydrogen fuel cell catalyst layer has been analysed after electrochemical cycling, in measurements performed at the Canadian Light Source (beamline 10ID1) and the Advanced Light Source (beamline 5.3.2.2) (Martens *et al*., 2020). Furthermore, the changing electrochemical state of a material can be studied *in situ* and *operando*, with control of applied potential, type of electrolyte, and electrolyte flow rate (Hitchcock *et al*., 2021).

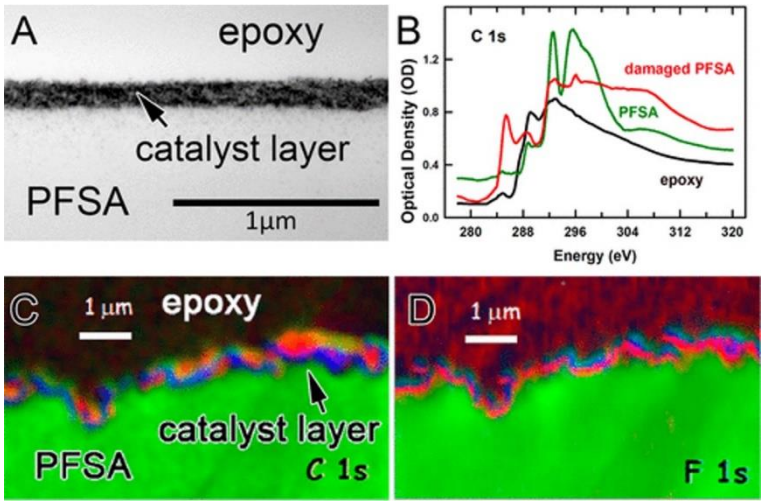

Figure 4.8. STXM cross-section images (chemical maps, bottom) showing the fuel cell catalyst layer after electrochemical ageing: undamaged PFSA (green), electrochemically damaged PFSA (red), and Pt (blue) (Martens *et al*., 2020).

Polymer electrolyte membrane fuel cells (PEMFCs) are a promising sustainable alternative to internal combustion engines for automotive applications. The ability to visualize the different components of PEMFCs will be transformative with respect to their optimization. Measurements such as those performed at the Advanced Light Source (beamline 11.0.2) using spectroscopic scanning coherent diffraction imaging (spectro-ptychography and spectro-ptychographic tomography) have enabled PEMFC cathode catalyst layers to be imaged quantitatively in both two and three dimensions, achieving 2D spatial resolution of better than 15 nm (Wu *et al*., 2018).

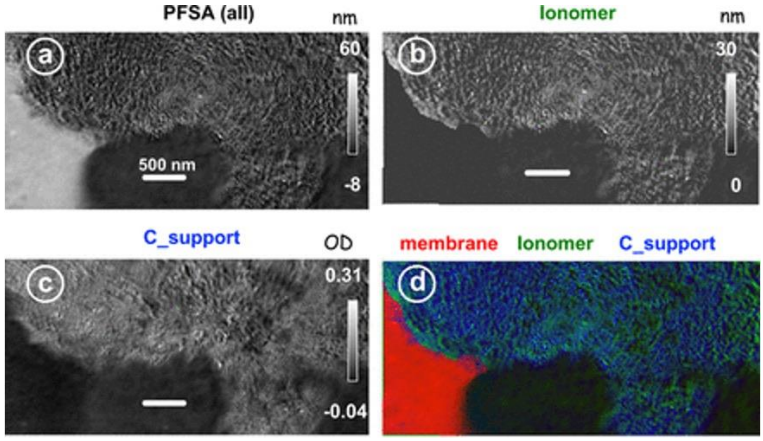

Figure 4.9. Ptychography of a PEMFC cathode: a) PFSA component map; b) ionomer map in the cathode region; c) map of nonfluorine components (mainly carbon support); d) composite of component maps of membrane (red), ionomer (green), and carbon support (blue) (Wu *et al*., 2018).

STXM and ptychography at the SoftiMAX beamline will allow direct mapping of chemical composition and morphology of such nanoscale interfaces. This can allow, for example, the optimization of catalyst layer architectures and structural properties for enhanced reaction processes and durability.

SM 2: iii | c, d: Efficient carbon capture could revolutionize many industries and allow for net negative CO_2 emissions. One interesting material for the capture of CO_2 is magnesium carbonate cement. STXM can be used to help understand the reaction mechanisms through characterization of cement particle structure and chemical state.

4.4 ForMAX

ForMAX allows *in situ* multiscale structural characterization from nanometre to millimetre length scales by combining full-field tomographic imaging, small- and wide-angle X-ray scattering (SWAXS), and scanning SWAXS imaging – in a single instrument. It is specially designed with a focus on advanced studies on wood-based materials. Full-field microtomography will allow both absorption contrast and propagation-based phase contrast 3D imaging, covering length scales from a few millimetres down to one micrometre. Scanning SWAXS imaging will allow to probe structures at length scales from several nanometres to several hundreds of nanometres.

Ongoing development: Scanning SAXS imaging and SAXS tensor tomography.

FM 1: i | c, d, e & ii | c, d, e: Thick electrodes are appealing for use in high energy density devices but succumb to sluggish charge transfer kinetics and poor mechanical stability. Nanomaterials with large aspect ratio such as carbon nanotubes represent a costly solution. Alternatively, electrodes based on a conductive cellulose nanofiber (CNF) network design with an interconnected pore network and compact structure offer a promising strategy for high-performance energy storage devices (Kuang *et al*., 2018).

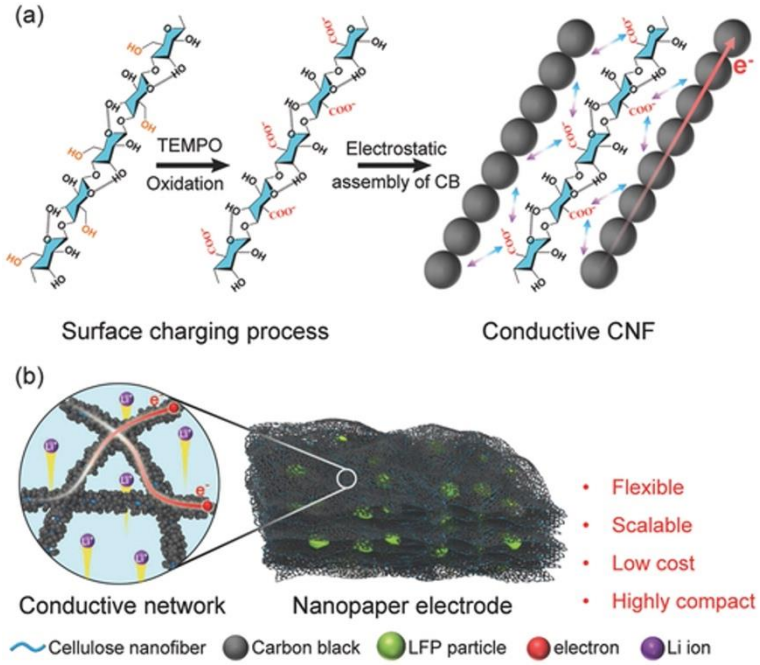

Figure 4.10. Showing the preparation and hierarchical network structure of a compact nanopaper electrode based on conductive nanofiber network (Kuang *et al*., 2018).

MXene aerogels are a promising class of two-dimensional materials for electrochemical energy storage and advanced composites. They are lightweight with high porosity, and exhibit rich elemental composition, surface chemistry, and excellent electrical conductivity. In order to translate these properties into high performance devices, it is essential to develop fabrication strategies that allow MXenes to be assembled into electrodes with tunable architectures, and then to be able to investigate the effect of their pore structure on capacitive performance. Compressive deformation enables the nano- and microstructure of lamellar freeze-cast aerogels to be tailored towards desired properties with a 3D structure of closely spaced, aligned sheets. Phase contrast X-ray microtomography allows

quantitative characterization of their microstructural evolution, required for optimizing manufacturing, understanding in-service structural changes, and determining how aerogel structure relates to functional properties, as illustrated by measurements performed at beamline ID15A at the ESRF (Bayram *et al*., 2020).

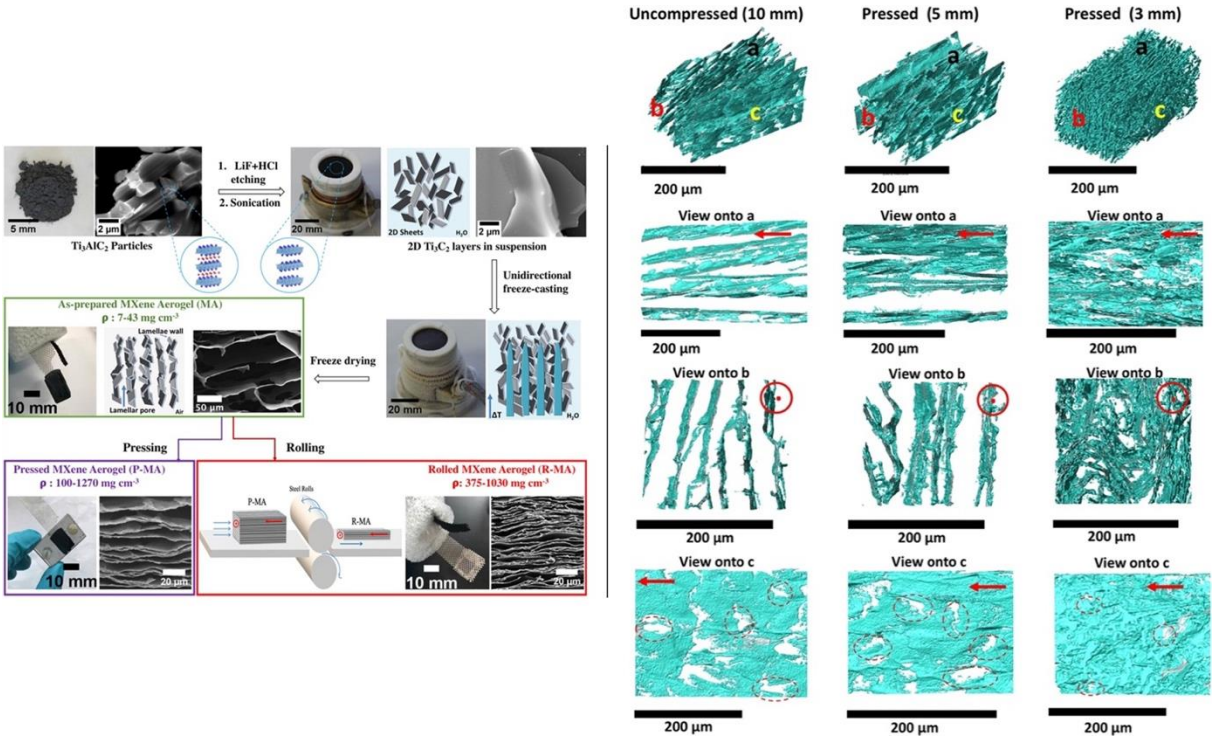

Figure 4.11. (Left) Fabrication strategy to produce $Ti_3C_2T_X$ aerogels and supercapacitor electrodes: as-prepared MXene aerogel (MA), pressed (P-MA), and rolled aerogel (R-MA). (Right) X-ray microtomography characterization of MA (uncompressed) and P-MA, showing alignment of sheets and the lamellar architecture (Bayram *et al*., 2020).

FM 2: ii | c, d & iii | c, d: Structural characterization techniques are fundamental to correlate the material macro-, nano-, and molecular-scale structures to their macroscopic properties and to engineer hierarchical materials. Using scanning small- and wide-angle X-ray scattering (sSWAXS) it is possible to investigate ultraporous and lightweight biopolymer-based foams using cellulose nanofibrils (CNFs) as building blocks. Such measurements performed at the cSAXS beamline at the Swiss Light Source have demonstrated the power of multimodal sSWAXS for multiscale structural characterization of self-assembled CNFs, through spatially resolved maps at the macroscale (foam density and porosity), at the nanoscale (foam structural compactness, CNF orientation in the foam walls, and CNF packing state), and at the molecular scale (cellulose crystallite dimensions) (Lutz-Bueno *et al*., 2022).

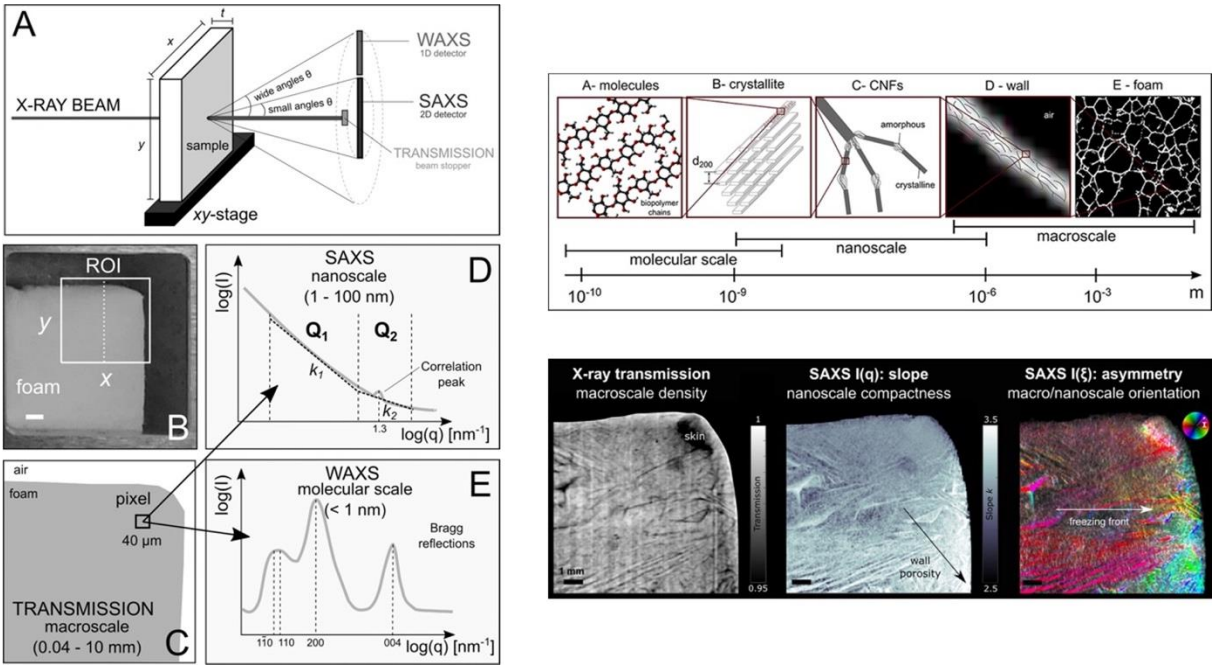

Figure 4.12. (Left) Schematic of a scanning X-ray scattering experiment. (Right top), definition of the multiscale hierarchical structure of CNF-based foams. (Right bottom), maps of relative transmission, SAXS signal, and structural orientation (Lutz-Bueno *et al*., 2022).

Scanning SWAXS imaging at the ForMAX beamline will allow for multimodal, multiscale structural characterization of hierarchical materials in a similar way, but importantly in combination with X-ray microtomography to provide 3D imaging at the macro- and microscopic level.

4.5 DanMAX (Imaging)

DanMAX is a materials science beamline dedicated to *in situ* and *operando* experiments. As described above the beamline offers two techniques: full field imaging, and powder X-ray diffraction and scattering (see section above). The imaging instrument will use a range of modalities, e.g. phase, absorption, and diffraction contrast. The full field microtomography will allow both absorption contrast and propagation-based phase contrast 3D imaging, with spatial resolution down to 1 µm.

Future development: Diffraction contrast tomography for reconstruction of 3D crystallographic microstructure (so-called 'grain mapping').

DM 1: ii | c, d: Understanding damage mechanisms in composite materials, such as glass or carbon fibre reinforced polymer (GFRP, CFRP), is important for their use in aerospace and automotive industries. In particular, characterizing fatigue damage in these materials for applications in wind turbines is of particular importance due to the very large number of loading cycles the rotor blades undergo during service. Using X-ray microtomography in a time-lapse manner (*in situ* or *ex situ*), it is possible to follow the relationship between local fibre distribution and crack propagation in three dimensions with regards to mechanical fatigue properties (Wang *et al*., 2018).

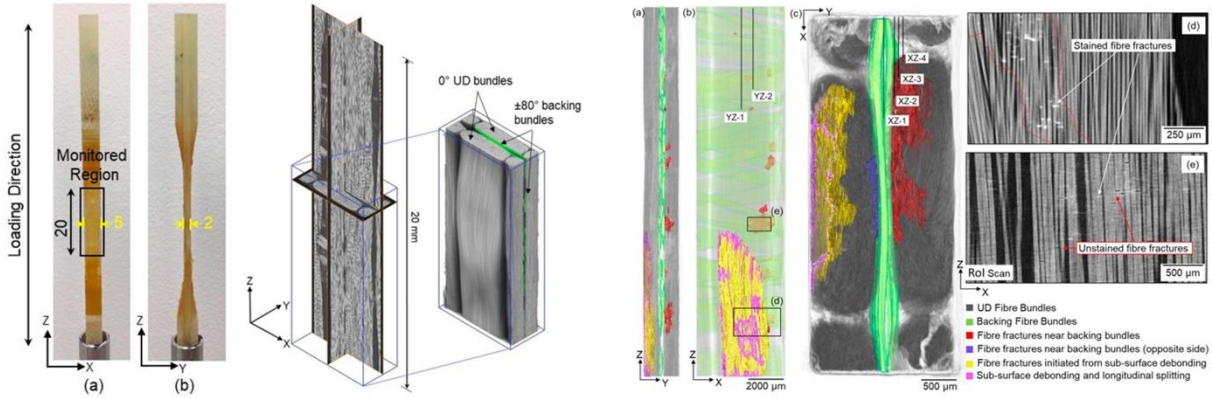

Figure 4.13. (Left) GFRP specimen and virtual X-ray tomography sections showing the fibre architecture. (Right) X-ray tomography characterization of fatigue damage after 500,000 loading cycles, visualizing fibre fractures, longitudinal splitting and debonding (Wang *et al*., 2018).

DM 2/FM 3: i | c, d & ii | c, d: The transport of substances dissolved in liquids and their chemical reactions in topologically complex environments such as porous media play an important role in applications such as geothermal energy production and catalysis. Time resolved X-ray tomographic microscopy provides the means to advance the investigation of, for example, solute transport through porous media at the pore-scale, as shown by measurements performed at the TOMCAT beamline, Swiss Light Source (Marone *et al*., 2020).

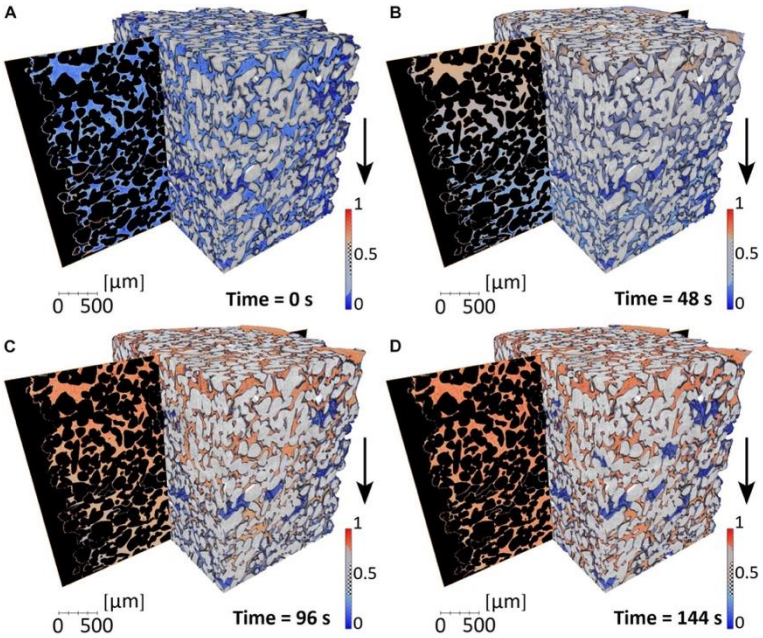

Figure 4.14. Time series of 3D tomographic datasets (with phase contrast) during the solute transport through a porous medium. The colour scale blue to red represents smaller to higher solute concentrations (Marone *et al*., 2020).

References

Ali-Löytty, H., *et al.,* 2022, MAX IV Experimental report 20200386 at HIPPIE beamline.

Anker, A. S., *et al.,* 2022, npj Comput. Mater. **8,** 213. https://doi.org./10.1038/s41524-022-00896-3

Bayram, V., *et al*., 2020, ACS Appl. Energy Mater. **3**, 411–422. https://doi.org/10.1021/acsaem.9b01654

Boix, V., *et al.,*2022, ACS Catal. **12,** 9897-9907. https://doi.org/10.1021/acscatal.2c00803

Bone, S.E., H.-G. Steinrück, and M.F. Toney, 2020, Joule **4,** 1637-1659. https://doi.org/10.1016/j.joule.2020.06.020

Broge, N. L. N., et al., 2022, Chem. Mater., **35,** 144–153. https://doi.org/10.1021/acs.chemmater.2c02842

D. Chakraborty, et al., 2022, J. Phys. Chem. C **126,** 16194. https://doi.org/10.1021/acs.jpcc.2c05213

Christensen, C. K., *et al.*, 2023, J. Synchr. Rad. **30.** https://doi.org/10.1107/S160057752300142X

D'Acunto, G., *et al.,* 2020, ACS Appl. Electron. Mater. **2,** 3915-3922. https://doi.org/10.1021/acsaelm.0c00775

D'Acunto, G. *et al.*, 2022, Faraday Discuss. **236,** 71-85, https://doi.org/10.1039/D1FD00116G

Divins, N. J., *et al.,* 2021, Nat. Commun. **12,** 1435. https://doi.org/10.1038/s41467-021-21604-7

Frank, S., *et al.,* 2021, J. Mater. Chem. A **9,** 26298-26310. https://doi.org/10.1039/D1TA06564E

Gjørup, F. H., P. Shyam, A. Povlsen, M. Mørch, J. Svane, T. O. Kessler, A. Schökel, M. R. Jørgensen, and Mogens Christensen, 2022, "A High-temperature Furnace for Millisecond Time-resolved Diffraction". *In preparation.*

Graae, K. V., *et al.*, 2023, J. Power Sources **570,** 232993. https://doi.org/10.1016/j.jpowsour.2023.232993

J. B. Grinderslev, *et al.,* 2022, Dalton Trans. **51,** 15806-15815. https://doi.org/10.1039/d2dt02513b

Guénet, H., *et al.,* 2017, Environ. Sci.: Nano **4,** 938-954. https://doi.org/10.1039/C6EN00589F

Hammarberg, S., *et al.,* 2020, Nano Res. **13,** 2460-2468. https://doi.org/10.1007/s12274-020-2878-6

Hitchcock, A.P., *et al*., 2021, Microscopy and Microanalysis **27**(S2), 59–60. https://doi.org/10.1017/S1431927621013295

Jarnac, A., *et al.,* 2017, Struct. Dyn. **4,** 051102. https://doi.org/10.1063/1.4993730

Jensen, M., *et al.*, 2021, J. Synch. Rad. **28**, 64-70. https://doi.org/10.1107/S1600577520014599

Juelsholt, M., *et al.,* 2021, Nanoscale **13,** 20144-20156. https://doi.org/10.1039/D1NR05991B

Jurgilaitis, A., *et al.,* 2014a, Nano Lett. **14,** 541-546. https://doi.org/10.1021/nl403596b

Jurgilaitis, A., *et al.,* 2014b, Struct. Dyn. 1**,** 014502. https://doi.org/10.1063/1.4833559

Jurgilaitis, A., Pham, T., Kroon, D., Ekstrom, C., Svensson, J., Wernersson, L.-E., Larsson, J., "Real-time investigation of fast phonons in semiconductor nanowires". *In preparation.*

Kahnt, M., *et al*., 2020, J. Appl. Cryst. **53**, 1444–1451. https://doi.org/10.1107/S160057672001211X

Källquist, I., *et al.,* 2021, ACS Appl. Mater. Interfaces **13,** 32989-32996. https://doi.org/10.1021/acsami.1c07424

Källquist, I., *et al.,* 2022, ACS Appl. Mater. Interfaces **14,** 6465-6475. https://doi.org/10.1021/acsami.1c12465

Karakachian, H., *et al.,* 2022, Adv. Funct. Mater. **32,** 2109839. https://doi.org/10.1002/adfm.202109839

Kim, J., *et al.,* 2018, J. Appl. Phys. **123,** 245103. https://doi.org/10.1063/1.5030178

Kirschner, J., *et al.,* 2021, Phys. Chem. Chem. Phys. **23,** 11568-11578. https://doi.org/10.1039/D0CP06387H

Kløve, M, *et al.,* 2022, Chem. Sci. **13,** 12883-12891. https://doi.org/10.1039/D2SC04522B

Knudsen, J., *et al.,* 2021, Nat. Commun. **12,** 6117. https://doi.org/10.1038/s41467-021-26372-y

Kokkonen, E., *et al.,* 2022, Rev. Sci. Instrum. **93,** 013905. https://doi.org/10.1063/5.0076993

Kong, X., *et al.,* 2022, Environ. Sci.: Atmos. **2,** 137. https://doi.org/10.1039/D1EA00092F

Kuang, Y., *et al*., 2018, Adv. Energy Mater. **8,** 1802398. https://doi.org/10.1002/aenm.201802398

Larsson, A. *et al.,* 2022, J. Alloys Compd. **895,** 162657. https://doi.org/10.1016/j.jallcom.2021.162657

Larsson, A. et al., 2022, Appl. Surf. Sci. **611,** 155714 https://doi.org/10.1016/j.apsusc.2022.155714

Li, H., *et al.,* 2020, ACS Nano **14,** 1905-4915. https://doi.org/10.1021/acsnano.0c00986

Li, J. *et al*., 2022, Adv. Energy. Mater **11,** 2003460. https://doi.org/10.1002/aenm.202003460

Lin, J. J., *et al.,* 2021, Atmos. Chem. Phys. **21,** 4709-4727. https://doi.org/10.5194/acp-21-4709-2021

Lorenc, M., Janod, E., Trzop, E., Mandal, R., Volte, A., Cailleau, H., Babich, D., Tranchant, J., Corraze, B., Cario, L., Iwai, S., Amano, T., Itoh, H., Kawakami, Y., Pham, T., Jurgilaitis, A., Kroon, D., Ekstrom, C., Larsson, J., "Comprehensive temperature study of strain wave-driven transition in nanocrystals of Ti_3O_5". *In preparation.*

Lutz-Bueno, V., *et al*., 2022, Biomacromolecules **23**, 676–686. https://doi.org/10.1021/acs.biomac.1c00521

Maibach, J., *et al.,* 2019, Nat. Commun. **10,** 3080. https://doi.org/10.1038/s41467-019-10803-y

Maison, A. *et al.*, 2000, Environ. Sci. Technol. **34,** 3242-3246. https://doi.org/10.1021/es9911418

Marçal, L., *et al.,* 2020, ACS Nano **14,** 15973-15982. https://doi.org/10.1021/acsnano.0c07426

Martens, I., *et al*., 2020, ACS Catal. **10**, 8285–8292. https://doi.org/10.1021/acscatal.0c01594

Mingo, N, and D.A. Broido, 2004, Phys. Rev. Lett. **93,** 246106. https://doi.org/10.1103/PhysRevLett.93.246106

Mochizuki, T., *et al.,* 2014, ChemSusChem **7,** 729-733. https://doi.org/10.1002/cssc.201301322

Näslund, L-Å., *et al.,* 2021, 2D Mater. **8,** 045026. https://doi.org/10.1088/2053-1583/ac1ea9

Ottesen, M, M. Goesten, I. Kantor, M. R. V. Jørgensen, and M. Bremholm, 2022, "Investigation of Dirac-like LaCuO3 with temperature and pressure". *In preparation.*

Ottesen, M, E. E. Petersen, C. H. Kronbo, F. Baudelet, L. Nataf, I. *Kantor*, M. R. V. Jørgensen, and M. Bremholm, 2022, "Pressure-induced charge-transfer and structural transition in hexagonal multiferroic HoMnO3". *Submitted.*

Pan, Y., *et al.,* 2022, Nat. Mater. **21,** 203-209. https://doi.org/10.1038/s41563-021-01149-2

Patera, L., *et al.*, 2023, Angew. Chem. Int. Ed. **62,** e202213295. https://doi.org/10.1002/anie.202213295

Povia, M., *et al.,* 2018, ACS Catal. **8,** 7000-7015. https://doi.org/10.1021/acscatal.8b01321

Puebla, J., *et al.,* 2020, Commun. Mater. **1,** 24. https://doi.org/10.1038/s43246-020-0022-5

Rissler, J., *et al.,* 2020, Energy Fuels **34,** 14505-14514. https://doi.org/10.1021/acs.energyfuels.0c02226

Roelsgaard, M., *et al.*, 2023, J. Appl. Cryst. **56,** https://doi.org/10.1107/S1600576723002339

Saketh Ram, M., *et al.,* 2021, Nature Electron. **4.,** 914-920. https://doi.org/10.1038/s41928-021-00688-5

Sandar Htet, C., *et al.,* 2022, Phys. Rev. B. **105,** 174113. https://doi.org/10.1103/PhysRevB.105.174113

Scardamaglia, M., *et al.*, 2021, Carbon **171,** 610. https://doi.org/10.1016/j.carbon.2020.09.021

Shavorskiy A., *et al.*, 2021, *ACS Appl. Mater. Interface, 13, 47629, https://doi.org/10.1021/acsami.1c13590*

Shyam, P, F. H. Gjørup, M. I. Mørch, A. Poulsen, I. Kantor, M. R. V. Jørgensen, and M. Christensen, 2022, "Sintering in seconds, elucidated by millisecond *in situ* diffraction". *Submitted.*

Svanström, S., *et al.,* 2022, ACS Mater. Au **2,** 301-312. https://doi.org/10.1021/acsmaterialsau.1c00038

Temperton, R. H., *et al.,* 2021, J. Chem. Phys. **154,** 234707. https://doi.org/10.1063/5.0050531

Tsao, C.-S., *et al.,* 2007, J. Am. Chem. Soc. **129,** 15997-16004. https://doi.org/10.1021/ja0752336

Tsukimura, K., and M. Suzuki, 2020, J. Appl. Crystallogr. **53,** 197-209. https://doi.org/10.1107/S1600576719017266

Wang, Y., *et al*., 2018, Materials **11**, 2340–2350. https://doi.org/10.3390/ma11112340

Wang, X., *et al.,* 2020, Phys. Rev. Lett. **124,** 105701. https://doi.org/10.1103/PhysRevLett.124.105701

Weber, S., *et al*., 2022, Adv. Sci. **9**, 2105432. https://doi.org/10.1002/advs.202105432

Weststrate, C. J., *et al.,* 2020, Nat. Commun. **11,** 750. https://doi.org/10.1038/s41467-020-14613-5

Wu, J., *et al*., 2018, J. Phys. Chem. C **122**, 11709–11719. https://doi.org/10.1021/acs.jpcc.8b02933

Wu, Z., *et al.,* 2021, Phys. Rev. Lett. **127,** 067002. https://doi.org/10.1103/PhysRevLett.127.067002

Yang, D., *et al.,* 2020, Adv. Sci., **7,** 2001117. https://doi.org/10.1002/advs.202001117

Xia, X., *et al.,* 2021, Nat. Commun. **12,** 6226. https://doi.org/10.1038/s41467-021-26510-6

Zalden, P., *et al.,* 2019, Science **364,** 1062-1067. https://doi.org/10.1126/science.aaw1773